PARTS OF THE ORIGINAL DOCUMENT

ARE OF POOR REPRODUCTIVE QUALITY

CERTAINES PARTIES DU DOCUMENT ORIGINAL

SONT DE PIÈTRE QUALITÉ DE REPRODUCTION

ENERGY, MINES AND RESOURCES

TITLE

DEVELOPMENT OF ADVANCED CERAMIC COMPOSITES BASED ON BORON NITRIDE FIBRES (UP-E-212)

Final Report by :

Dr.D.Ghosh, Dr.J.K.Jacobs, Dr.P.Lucuta and Dr.S.Das Gupta
The Electrofuel Manufacturing Company Limited

Work on the project was conducted under the auspices of the
Canada Centre for Minerals and Energy Technology,
Energy, Mines and Resources, Canada

DSS File No.	:	06SQ.23440-5-9226
DSS Contract Serial No.	:	1SQ.85-00242
CANMET Project No.	:	302905
CANMET Scientific Authority	:	Dr.T.A.Wheat
Dated	:	15th November 1987

THE ELECTROFUEL MANUFACTURING CO.
9 Hanna Avenue, Toronto, Ontario, Canada M6K 1W8 Tel. (416) 535-1114 Fax. (416) 535-2361

ENERGY, MINES AND RESOURCES.

TITLE: DEVELOPMENT OF ADVANCED CERAMIC COMPOSITES BASED ON BORON NITRIDE FIBRES (UP-E-212).

Final Report by:

Dr. D.Ghosh, Dr. J.K.Jacobs, Dr. P.Lucuta and Dr. S.Das Gupta.
The Electrofuel Manufacturing Company,
9, Hanna Avenue, Toronto, Ont. M6K 1W8.

Work on the project was conducted under the auspices of the Canada Centre for Minerals and Energy Technology, Energy, Mines and Resources Canada.

DSS File No: 06SQ.23440-5-9226.
DSS Contract Seriel No. 1SQ85-00242
CANMET Project No. 302905
CANMET Scientific Authority: Dr. T.A.Wheat.

Date: 15th November 1987.

117 pp

MICROMEDIA

TABLE OF CONTENTS.

1.	Summary.	1
2.	Introduction.	4
	2.1 Boron Nitride.	6
	2.2 Boron Nitride Fibres.	9
	2.3 Particulate composites.	11
	2.4 Applications.	12
	2.4.1 Ceramic Break Ring.	15
	2.4.2 Ceramic Boats for Al metallizing.	18
	2.5 Program Objectives.	19
3.	Characterization of Materials.	20
	3.1 Boron Nitride powder	20
	3.1.1 Boron oxide content.	20
	3.1.2 Structural Characterization	21
	3.1.3 Microscopy.	27
	3.1.4 Thermal Treatment.	29
	3.2 Boron Nitride Fibre.	32
	3.2.1 X-Ray diffraction Analysis.	32
	3.2.2 Microscopy.	37
	3.2.3 Boron Oxide content.	42
	3.3 Other Powders	44
	3.3.1 Titanium diboride.	44
	3.3.2 Aluminum Nitride.	49
4.	Processing.	50
	4.1 Powder Preparation.	50
	4.2 Blending.	51
	4.3 Cold Pressing.	52
	4.4 Hot Pressing.	65
	4.4.1 Mold Design	67
	4.4.2 Kinetics of hot pressing.	77
5.	Finished Part Characteristics.	82
	5.1 Monolithic Boron Nitride.	82
	5.1.1 Structural Analysis	82
	5.1.2 Microscopy	87
	5.1.3 Strength.	91
	5.2 BN/BN Composite.	93
	5.3 Particulate Composites.	99
6.	Conclusions.	114

1. SUMMARY

The following is a description of the work undertaken under contract entitled " Development of Advanced Ceramic Composites Based on Boron Nitride Fibres ". Under this contract, The Electrofuel Manufacturing Company carried out research and technology development in the area of advanced ceramic-ceramic composites, with emphasis on the use of Electrofuel's unique Boron Nitride Fibre manufacturing capability.

For the evaluation of the characteristics and potential of ceramic composites based on Boron Nitride, the investigation was done at three levels :

* Concept Evaluation
* Technology Development
* Product Development

Beyond the preliminary work of evaluating a number of concepts for tailoring the electrical and mechanical properties of Boron Nitride, the technology development involved characterization of

the starting materials, process development and of course measurements of finished part characteristics. This work, coupled with market requirement analysis, supported the final leg of product development.

With the massive growth on advanced materials, there is an increasing interest in developing ceramic/ceramic composites. Such composite development is being pushed from both mechanical strength and fracture considerations and also from certain thermal and electrical property requirements. Material properties can often be tailored to specific market requirements. Work of this type has been highly successful in the oxide ceramic area and is, as expected, equally significant with non-oxide ceramics such as Boron Nitride.

Several Boron Nitride composite materials produced had valuable properties which are currently being applied to specific products. These properties include :

* Enhanced strength and thermal shock
* Enhanced high temperature strength
* Tailored electrical resistivity
* Enhanced anisotropy of properties
* Improved hardness
* Improved wear resistance

In addition, the basic understanding of properties and processing of boron nitride itself was greatly advanced as a by-product of the analysis of its behaviour with specific additives.

The product opportunities for these new composites are considerable. Application areas currently under investigation include :

* Ceramic substrates
* Furnace elements
* Electrochemical electrodes
* Aluminum evaporator boats
* HCC break rings
* Grinding and polishing media
* Thermocouples.

A number of spin-offs from the program are an additional unexpected development. They include :

* Hot press die technology
* Powder purification technology

As these and other spin-offs emerge, they will be evaluated for rapid commercialization.

2. INTRODUCTION

The current surge of international interest in Advanced Ceramics is related to the huge global market (and market potential) for these materials. Groups in Japan, the USA and elsewhere have identified this field as one of national strategic importance and a recent study in Canada (Murthy/DRIE) has come to a similar conclusion. Recognition is also developing that Advanced Ceramics hold the key not only for the growth of present day industries but, more importantly, for the creation of new industry. Developments in this field tend to have a catalytic effect and generate positive sectoral impacts on other key industries of Canada such as electronics, steel, transportation and energy.

Traditional ceramics have long been based on artful and effective mixtures of natural materials such as clays and powdered rocks. Through ingeneous processing, these materials have yielded a wide variety of " synthetic rocks " with properties which have found major uses in industrial (and of course domestic) practices. These traditional ceramics are all complex mixtures, some components of which are useful, others detrimental. A generation ago, the first single component " pure " ceramics appeared, fabricated from industrial chemicals such as Al_2O_3, BeO, MgO, etc.

Over the years, increasing levels of purity and grain refinement were achieved, both for oxides and, later, non-oxide ceramics. Commensurate with these achievements came dramatic improvements in mechanical, electrical and chemical properties. It has been appreciated only rather recently that controlled addition of certain " impurities " to the monolithic pure ceramics could result in even more dramatic improvement of material properties. These impurities can be in the form of powders, fibres, chemicals in solution, etc.. and it is through an understanding of the pure monolithic ceramic and the chemical and physical effects of the individual impurities that the properties of the monolithic ceramic can be " tailored " to meet the needs of specific applications.

2.1 BORON NITRIDE

Boron Nitride (chemically BN) is a " pure" monolithic non-oxide ceramic with a significant world market and interesting physical and chemical properties. It is similar in structure to carbon : carbon atoms are alternately replaced by atoms of boron and nitrogen. Like carbon it can be formed in a number of structures :

* glassy, amorphous
* hexagonal, planar, graphite
* cubic, diamond structure

The electronic band structure of BN differs greatly from that of carbon and so whereas graphite is a conductor of electricity, boron nitride is an excellent electrical insulator (and thus white). Both diamond and cubic boron nitride exhibit extreme hardness and are both similarly formed by the simultaneous application of heat and pressure to the hexagonal (graphite) material.

The work on BN composites centres on the hexagonal structured material, with some use being made of low crystallinity structures. Like graphite, hexagonal BN is soft and readily machinable. It has great lubricity, but relatively low strength - not much better than that of graphite. Like graphite, BN is rather anisotropic in properties , but the mixed-orientation polycrystalline material is relatively homogeneous and isotropic. BN is useful for its high thermal conductivity, low thermal expansion, and great resistance to thermal shock. It remains solid to very high temperatures (> 2500 degrees C in nitrogen) and has strength and thermal conductivity which increase with temperature - again properties

similar to those of graphite. However, unlike graphite :

* BN is an electrical insulator even at high temperatures, with high dielectric strength, low dielectric constant, and low dielectric loss even at high temperatures and high frequencies.

* BN has low chemical reactivity, especially when hot. It does not react with molten iron, reacts very slowly with high temperature molten aluminum, is neither intercalated by alkali metals nor by transition metals, and is non reactive, even at high temperatures, to oxides such as alumina, silica, zirconia, etc.

It is largely these latter properties for which boron nitride is chosen over graphite in many applications in spite of its greater cost.

While the oxidation products of carbon are gasses (CO and CO_2), the oxidation product of boron nitride is a low melting glass, (B_2O_3). This glass is nearly always present in small quantities in otherwise pure boron nitride and can affect the properties of boron nitride and combine or react with many composite structure additives. Its presence must always be considered when evaluating the behaviour of additives to (or composites with) boron nitride. Typical properties of Electrofuel hot pressed Boron Nitride are as follows:

Typical properties of hot pressed BN:

Composition:	BN	95-97%
	B_2O_3	2-4 %
	Other	0.2-1 %
Density		2.0-2.1g/cm^3
Compressive Strength:	Parallel*	45,000 psi
	Perpendicular*	34,000 psi
Modulus of rupture, (Parallel *)	20°C	15,000 psi
	1350°C	3,000 psi
Modulus of Elasticity		9×10^6 psi
Coefficient of thermal expansion:	Parallel*	8×10^{-6}/°C
	Perpendicular*	0.77×10^{-6}/°C
Thermal conductivity at 300°C, (Cal/cm /sec/°C)	Parallel*	0.036
	Perpendicular*	0.069

(* to the pressing direction)

2.2 BORON NITRIDE FIBRES

Boron Nitride fibres, like carbon fibres, cannot be formed by conventional fibre forming techniques as the material melts and simultaneously decomposes at 3250°K. Hence an indirect method was developed for fibre production. Since Electrofuel is the only source for this material, it is expected that applications for this material will slowly evolve over a period of time as more and more people experiment with the material and the price of the material becomes less expensive.

Typically the fibre diameter is 3 microns. The manufacturing process can be modified to provide fibre diamter of 0.5 to 10 microns. For super insulation application, felts with fibre diameter of 1 micron is adequate.

The fibres are fine grained polycrystalline with high resistance to self abrasion and wear. The thermal stability of the fibres are due to the presence of the planar network of hexagonal rings similar to graphite and these rings are packed in such a way that multiple cleavage of bonds across the planar network is necessary for thermal decomposition. The high electrical resistivity derives from a complete lack of resonating electrons. The crystallites in the fibres are not oriented; hence the fibre properties do not possess any directional characteristics as is normally observed in the hot pressed Boron Nitride where partial orientation of crystallites occur during the production of solids.

From Table 1 it can be seen that BN fibres are intermediate modulus material, in between the high modulus fibres such as boron, graphite, SiC, B_4C etc., and the low modulus fibres such as nylon and rayon. BN fibres with tensile strength as high as 210,000 psi have been observed, which compares well with carbon fibres (50 - 100,000 lb/in^2). Typical range of BN fibre is however between 50,000 to 125,000 psi.

Table 1

Comparison of High Performance Fibres

	Fiber	Density	Diameter, μm	Modulus $X10^6$ lb/in^2
High-Modulus	B	2.4	80-100	60
	SiC	3.2	80-100	70
	B_4C	2.5	80-100	70
Graphite (oriented)		1.8-2.0	~7-9	60
Intermediate-Modulus	steel	7.8	4-50	20-30
	S-glass	2.5	12	12.4
	E-glass	2.6	5-15	10
	BN	1.8	4-6	6-10
Low-Modulus	nylon	1.1	10-40	0.40
	rayon	1.5	10-40	0.4

2.3 PARTICULATE COMPOSITES

The addition of foreign particulates into boron nitride during processing can have a major impact on its properties. As boron nitride is extremely non reactive, these foreign materials would be expected to reside as simple mixtures with BN, and for most materials this does seem to be the case. Some particulate additives react with residual B_2O_3, or each other, to affect the material's properties in a more complex way. In a few cases, direct reaction with BN is observed.

A number of particulate composites have been prepared and tested as a part of this and other work and a summary of some of the more interesting materials follows :

Particulate additive	Property improvement	Property deterioration
CaO	moisture absorbtion	strength
Al_2O_3	H.T.strength	electrical,machinability
Al	H.T.strength	electrical,machinability
SiC	wear resistance	machinability
SiO_2	strength	H.T.chemical resistivity and machinability

2.4 APPLICATIONS

Boron nitride solid has a wide range of applications for which it is the material of choice. In most (but not all) cases, some improvement of a particular property would increase the material's acceptability. The following table shows some of these applications and the most critical properties. There is considerable room for improving the product acceptability in most of these cases by preparing a composite tailored to that particular application. For example, H.T. gaskets and rotary seals might be compounded with a wear resistant additive (Al_2O_3, AlN, Si_3N_4, TiO_2, B_4C, TiB_2, etc.) without severely impacting other desirable properties (thermal shock resistance, thermal conductivity, high temperature resistance, machinability, etc.).

Application	Property in need of improvement
Electrical insulation in H.T. induction furnaces	H.T.strength
Neutron absorber	Neutron cross-section (isotropic purity)
H.T.gaskets and rotary seals	Wear resistance
Metal melting and filtering	H.T.strength
Glass and slag melting	Chemical resistance

Battery separators	Surface wettability
Heat sinks for electrical devices	R.T.strength, flexibility
Filter media.H.T.& biological	Chemical resistance
Ceramic boats for metallizing	H.T.corrosion.erosion
Break rings for HCC of steels	H.T.strength,wear resistance

Market size and speed of market acceptance will affect the priority with which one might address such " tailored materials ". In that regard, two of the most promising areas are the Break Ring for Horizontal Continuous Casting and the Aluminum Metallizing Boat.

Presently there are about a dozen HCC machines operating in the world: two in North America, one in Australia, five in Japan, four in Europe and one in S. Korea. Break rings are normally replaced after every heat, and hence, a two strand machine casting on the average six heats per day will require twelve rings per day, or 3600 rings per year, which at an average price of $150, amounts to $540,000 per year per machine.

More importantly it is a rapidly growing market as more and more mini-steel mills convert to this Horizontal Casting Process. With the development of an improved BN break ring, a major problem area in this HCC process will be resolved and we expect that material to be used in a substantial portion of the total market. From our discussion with NKK it appears about 10 or more mills will be installed in the next 24 months.

Metallized coatings, especially that of Aluminum on plastic, paper and other materials are a growing industry. Applications include the packaging of air tight food stuffs where the thin coating of Aluminum metal decreases the oxygen diffusion and reduces significantly the light induced oxidation, various high tech applications in aerospace industry and for decorative situations such as labels for beer bottles. The main growth of the industry is being driven by the high tech and food packaging business.

In the Aluminum metallizing process, a boat (6" x 0.25" x 1") typically costs $65 and lasts for about 10 hours of operation. During the metallizing process, a single machine will use about 10 boats per run, with the operation needing about 20 boats per day (3 shifts) or 100 boats per week. There are five companies in the Ontario-Quebec area carrying out this work and it is estimated that about 80 companies in North America are involved in Aluminum metallizing. The North American market is estimated to absorb about $24 million worth of ceramic boats and the world wide market is possibly about $60 Million.

2.4.1 CERAMIC BREAK RING

The horizontal continuous casting (HCC) of steel has several advantages over the conventional vertical continuous casting process (VCC), such as:

1. lower capital, construction and maintenance costs
2. better steel quality obtained as air oxidation of molten steel is avoided
3. wider variety of steel grades (including crack sensitive and aluminum containing steels) can be cast
4. lower labour cost and increased automation possible
5. round billets can be cast

For these reasons a number of mini steel plants (electric arc furnace-continuous caster-mini-mill) in North America, Japan, South Korea, Australia and Europe have installed the HCC process and a number of other mills (including two in Canada) are presently considering it. It appears this process will be a major growth in the steel industry and we understand from Nippon Kokan that they are presently setting up a number of these mills, which will be operational from 1987.

The HCC process is schematically shown in Figure 1. The molten steel from the ladle passes through the tundish into the water cooled copper mold, where it partially solidifies. The billet is continuously withdrawn and is further cooled by a spray of water in the secondary cooling zone. It is then cut into length by a synchronized gas torch cutter.

One of the components hindering the development of HCC for steel is a ceramic part known as the break ring, which forms a seal between the molten metal tundish and the water cooled copper mold (see Figure 2).

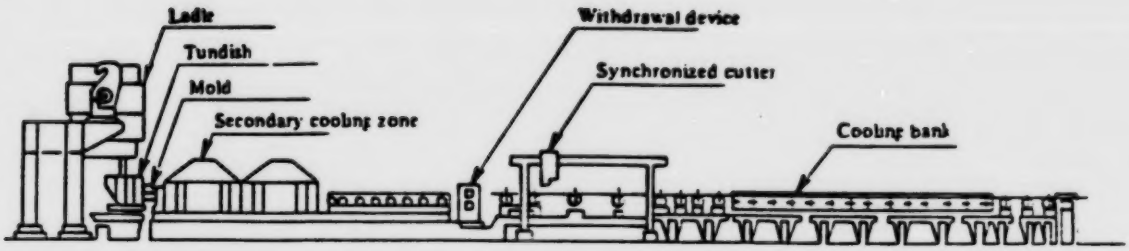

Fig. 1 Elevation of the HORICAST.

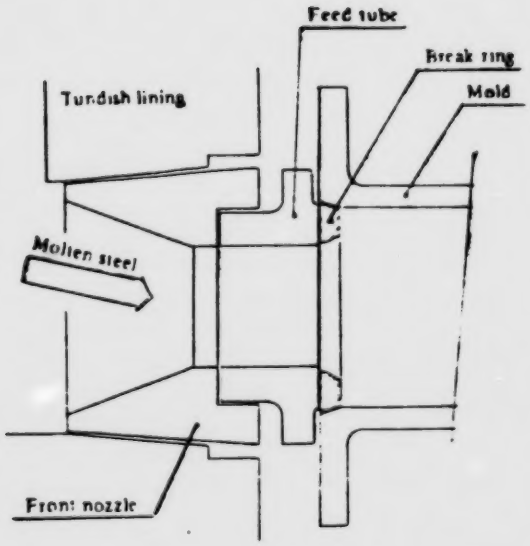

Fig. 2 Scheme of joint assembly between tundish and mold

The break ring is a critical component of the process and it must have a combination of chemical, mechanical and thermal properties, such as:

1. good chemical stability in contact with various grades of molten steel alloys at about 1550°C
2. good high temperature strength to withstand the large thermal stress generated by the sharp temperature gradient across the ring
3. good thermal shock resistance, as it is heated from room temperature to 1550°C instantaneously at the start of casting
4. good machinability, as an accurate joint to the mold has to be made
5. good erosion and abrasion resistance

Extensive discussions with personnel from Armco, Nippon Kokan and Steel Casting Engineering Company confirms that BN is the material of choice from thermal, chemical, and certain mechanical points of view.

2.4.2 CERAMIC BOATS FOR ALUMINUM METALLIZING

A continuous coating or metallizing of aluminum on paper, plastic films, etc. is commercially carried out by a vacuum evaporation technique. It consists of a vacuum chamber containing a number of ceramic boats, which are electrically heated to aluminum vaporizing temperature of 1400 - 1600°C. High purity Al wire is continuously fed into these boats at a rate at which Al is evaporating and coating the plastic film. The life of these boats is about 10 - 14 hours and they constitute a major consumable item of the process.

Presently a single metallizing machine typically consumes about 20 boats per day at an annual cost of about $300,000. Hence there is a major interest in increasing the life of these ceramic boats. Also, plant operators observe a considerable amount of failures due to initial thermal shock.

The ceramic boat must have the following combination of chemical, electrical and physical properties:

1. They must reasonably withstand molten aluminum, which is very corrosive at 1400° - 1600°C.
2. The electrical resistivity must be within the desired range. There should be very little local variation of this resistivity, otherwise failure due to uneven heating of the boat will occur.
3. Thermal shock resistance should be high to allow rapid heating or cooling from room temperature to 1400° - 1600°C.
4. Good machinability.
5. Good wetting by molten aluminum.

2.5 PROGRAM OBJECTIVES

With the perspective of a market opportunity and a manufacturing technology, a program of fundamental research, followed by technology development, was envisioned and embodied in the present contract. Thus the objectives are :

* Develop ceramic composites based on boron nitride, other particulates, and fibres, to augment the general understanding of these materials and to satisfy specific market needs.

* Develop hot pressing techniques to produce dense composite bodies.

* Develop the required ancillary technology to meet the above two objectives.

* Prove the technology with specific product-requirement testing.

3 CHARACTERIZATION OF MATERIALS

A first step in the development of any ceramic material, be it monolithic or composite, is the characterization of the starting materials. Such mundane questions as particle size, agglomerate size, crystal structure, etc., will be of vital importance to the properties of the finished product (unlike, for example, metals where such considerations are often irrelevant to the finished properties). As boron nitride itself is the matrix of all the composites studied, a characterization of the BN starting material is of utmost importance. An understanding of the other components of the composite is also needed, and each will be addressed in turn.

3.1 BORON NITRIDE POWDER

3.1.1 BORON OXIDE CONTENT

The BN powder composition is important for the properties of final boron-nitride products. This fact requires chemical analysis for each batch of powder, especially B2O3 determination.The B2O3 content in the BN powder was determined by the acid-soluble boron method and the optimum percentage range for the hot-pressing sintering process was found to be

3.1.2 STRUCTURAL CHARACTERIZATION

The X-ray diffraction technique was used for structural characterization of various BN powders. Two different BN powders were analysed in the first stage, both with the same chemical composition (B2O3 content) but with strikingly different behaviour during the hot-pressing. One was able to be sintered (active powder) while the other could not be sintered under any similar technological conditions (non-active powder).

Using Cu k_{α} radiation (Ni filter for k_{β} ; range 2×10^3 cps)the X-ray diffraction patterns of BN non-active and active powder were recorded in order to better understand the requirements of the initial starting powder for pressing into compacts (Fig.3.1).

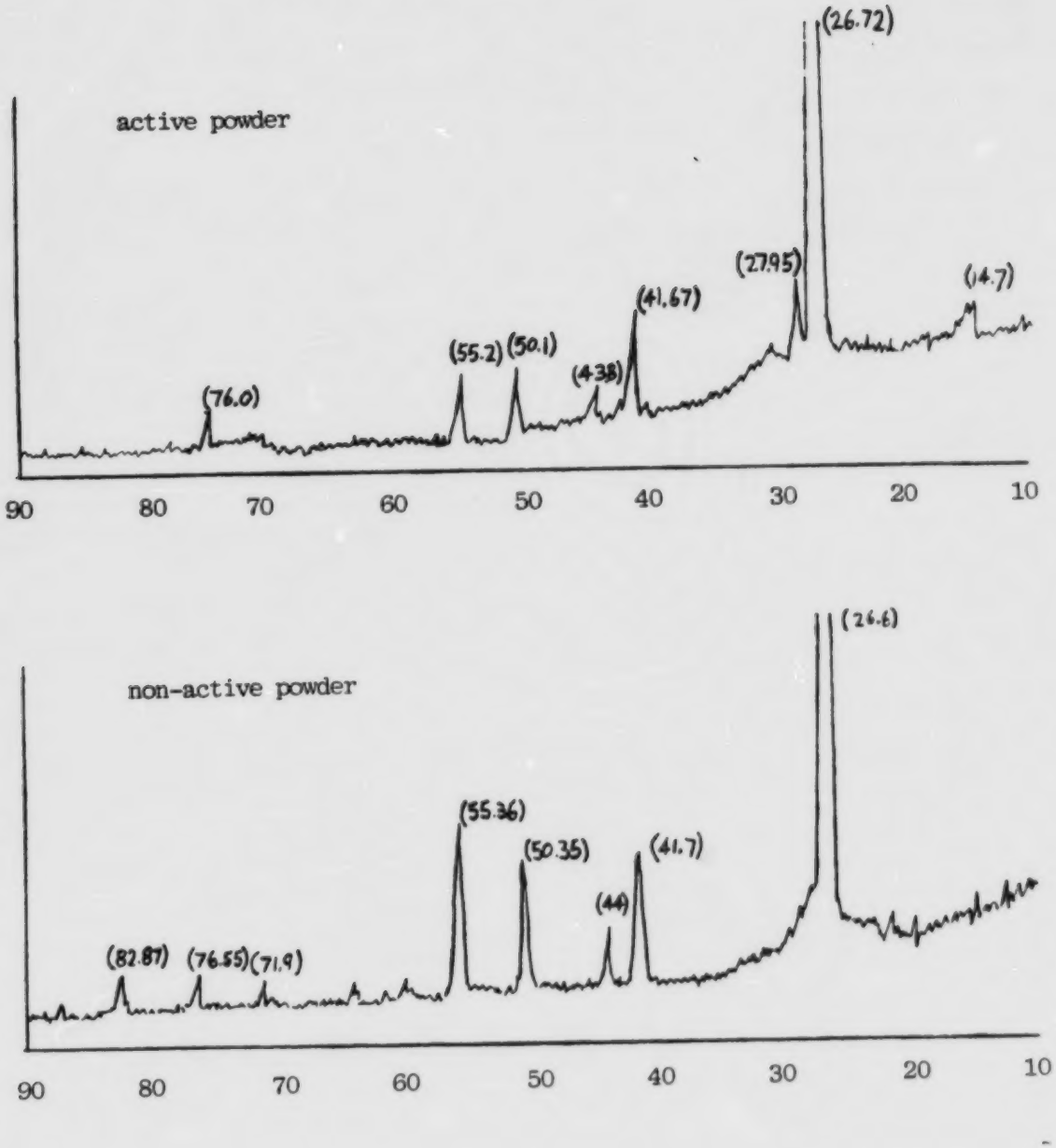

Figure 3.1 X-ray diffraction patterns of active and non-active BN powders

Both samples have a hexagonal structure and the experimental values of interplanar distances are well fitted by calculated values and with those listed by ASTM (Table 3.1).

Miller indices:	non-active BN powder		active BN powder		
hkl	dhkl exp.	dhkl calc.	dhkl exp.	dhkl calc.	dhkl ASTM
002	3.33	3.31	3.336	3.327	3.33
unidentified	-	-	3.196	-	-
100	2.160	2.157	2.167	2.1675	2.17
unidentified	-	-	2.147	-	-
101	2.058	2.054	2.066s	2.0617	2.06
102	1.8102	1.8100	1.8163s	1.8161	1.817
004	1.6560	1.6552	1.6639	1.6637	1.667
103	-	-	-	-	1.552
104	1.3130	1.3128	-	-	1.322
110	1.2445	1.2445	1.2514s	1.2514	1.253
112	1.1649	1.1649	1.1713	1.1713	1.173
105	-	-	-	-	1.138
006	1.1034	1.1034	-	-	1.111

TABLE 3.1 Interplanar distances from X-ray diffractions of BN non-active and active powder

The index "s" means splitting of the x-ray line which occurs in the pattern of active powder. This can be explained by structural defects like packing defects, parallel or rotational displacements (turbostratic defects) and by sp2-hybridization. These may also explain the peaks marked "unidentified" in table 3.1.

The lattice parameters have been determined from the interplanar distances using the relation:

$$\frac{1}{d^2_{hkl}} = \frac{4c^2(h^2+hk+k^2)+3a^2l^2}{3a^2c^2}$$

The (110) and (112) peaks were used to calculate the lattice parameters, whence the relation becomes:

$$a = 2d_{110} \qquad \text{and}$$

$$\frac{1}{c^2} = \frac{1}{4d^2_{112}} - \frac{1}{a^2}$$

The lattice parameter determination has shown that the "a" and "c" values are higher for the the active powder (a=2.503 Å; c=6.655 Å) compared to those obtained for the nonactive powder (a=2.489 Å; c=6.621 Å)

The data were checked by recording the X-ray pattern on film and the same values of interplanar distances were obtained. In the case of active BN powder, the film X-ray image has also shown the unidentified peaks and the above mentioned splittings.

The estimated lattice parameters give a volume (density) difference of 1.6%, a significant difference.

Another measure of the structural regularity for graphite-like materials is the " graphitization index ". It is defined as :

$$R = \frac{A(100)+A(101)}{A(102)}$$

where A(hkl) represents the area of the (hkl) peak from the diffraction pattern. The value is R=2.2 for the active powder and R=1.45 for the inactive powder. In fig.3.2 the recorded (100),(101) and (102) diffraction peaks for active and inactive powders are shown. The graphitization index of the structurally ordered BN is 1.6. The higher value of R for the active powder than for structurally ordered BN product again shows the presence of structural defects such as packing defects (which are formed due to weak bonds between layers), and parallel and rotational displacements of layers (in their planes) into arbitrary positions. This may explain the activity of the powder in sintering.

The smaller value of graphitization index and the smaller values of the lattice parameters obtained for inactive powder show a higher degree of crystallization (a graphite structure) without defects which could explain the inactivity of this powder in sintering.

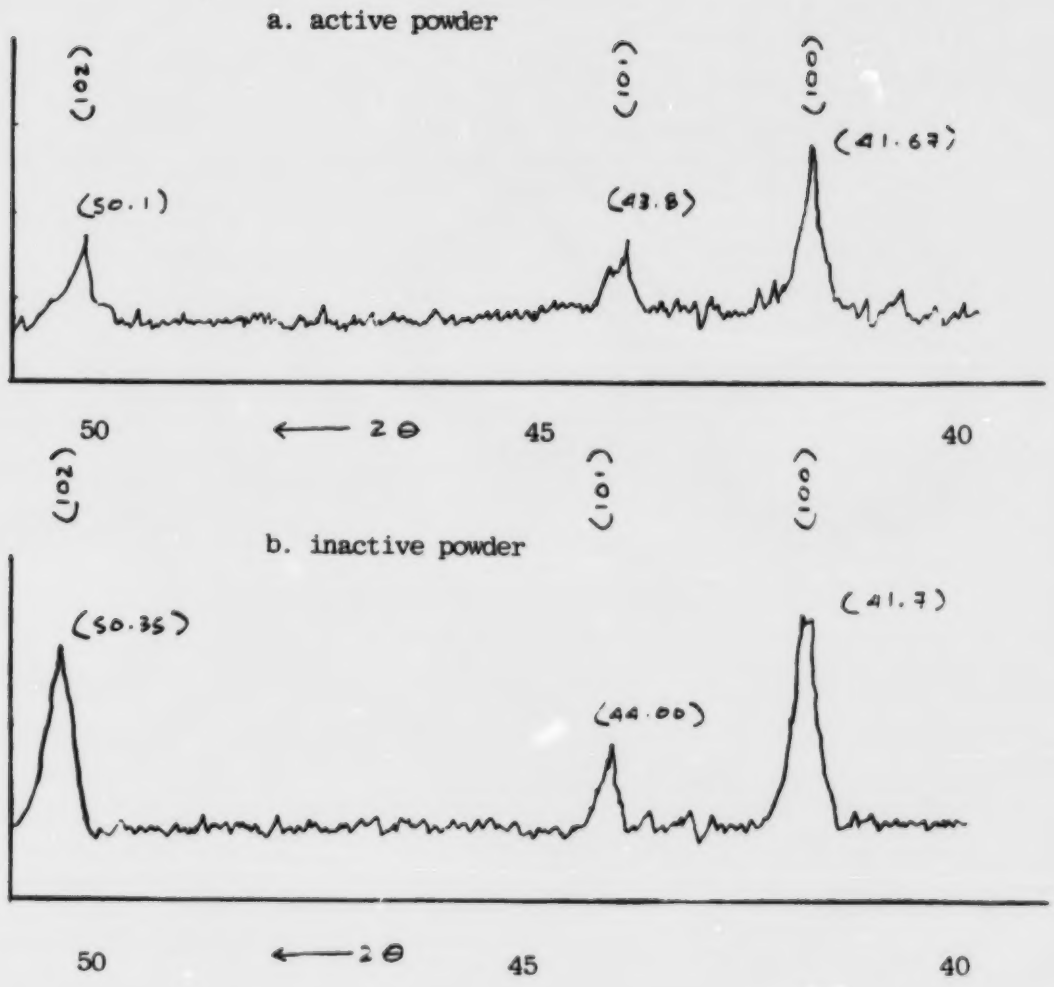

Fig.3.2 The X-ray diffraction pattern region showing (100),(101) and (102) peaks for a. active BB powder b. non-active BB powder from which was determined the graphitization index

3.1.3 MICROSCOPY

Using scanning electron microscopy, some structural features of BN powder (shape and particle size) were determined. The samples were prepared by dispersing the powder in carbon tetrachloride and covering with gold for conductivity and contrast. The secondary electron image of BN powder has shown a wide range of the grain size and the coalescence of the particles into agglomerates. (Fig.3.3 a,b).

The powder flows poorly (as one might expect from particle size) and agglomerates easily. Agglomerate sizes observed by optical microscopy varied in size from a few microns to as great as one millimeter. Small amounts of stirring, shaking, etc., are sufficient to form, break, and reform many of these soft agglomerates.

The BN particles are flakes which are difficult to disperse. Size is in the range: 0.2 μm to 5 μm, with particles having submicron dimensions predominating.

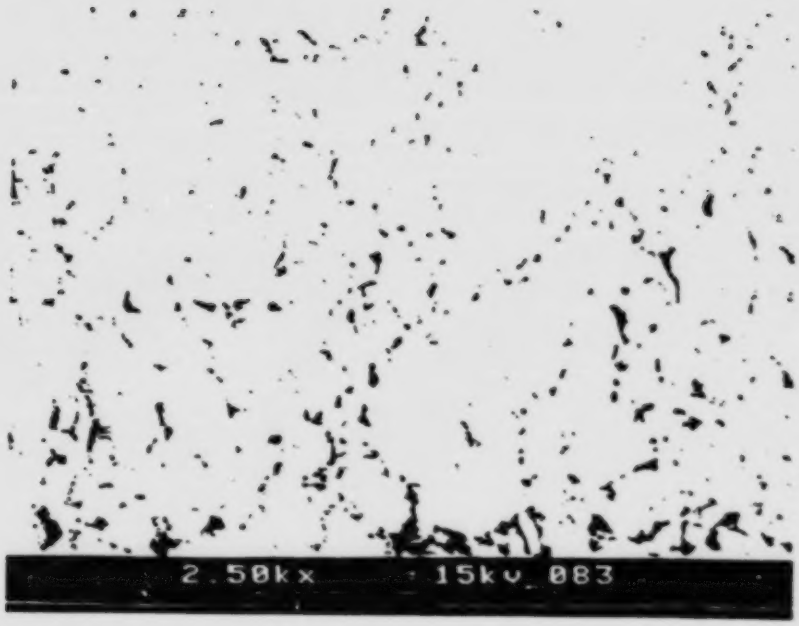

Fig.3.3a. Scanning electron image of BN active powder (x1,500)

Fig.3.3b Secondary electron image of BN active powder (x6,000)

3.1.4 THERMAL TREATMENT

In order to obtain a better understanding of BN non-active powder and the possibility for its transformation, the BN active powder was heated to 2400°C. in a nitrogen atmosphere.This heat treated BN powder was analysed using X-ray diffraction and scanning electron microscopy and the structural changes noted.

The X-ray diffraction patterns of active BN powder. before and after heat treatment. recorded under the same experimental conditions. are shown in Fig.3.4.

The x-ray diffraction patterns show some structural changes. The extra peaks and the splittings have disappeared after heat-treatment. The X-ray pattern of thermally treated active BN powder is similar to that of non-active BN powder.

The scanning electron microscopy shows no significant changes in the shape and size of BN flakes after heat-treatment. Secondary electron images of thermally treated BN powder, dispersed in carbon-tetrachloride and gold covered are given (Fig.3.5 a.b). The powder was more easily dispersed in this case and better contrast was obtained.

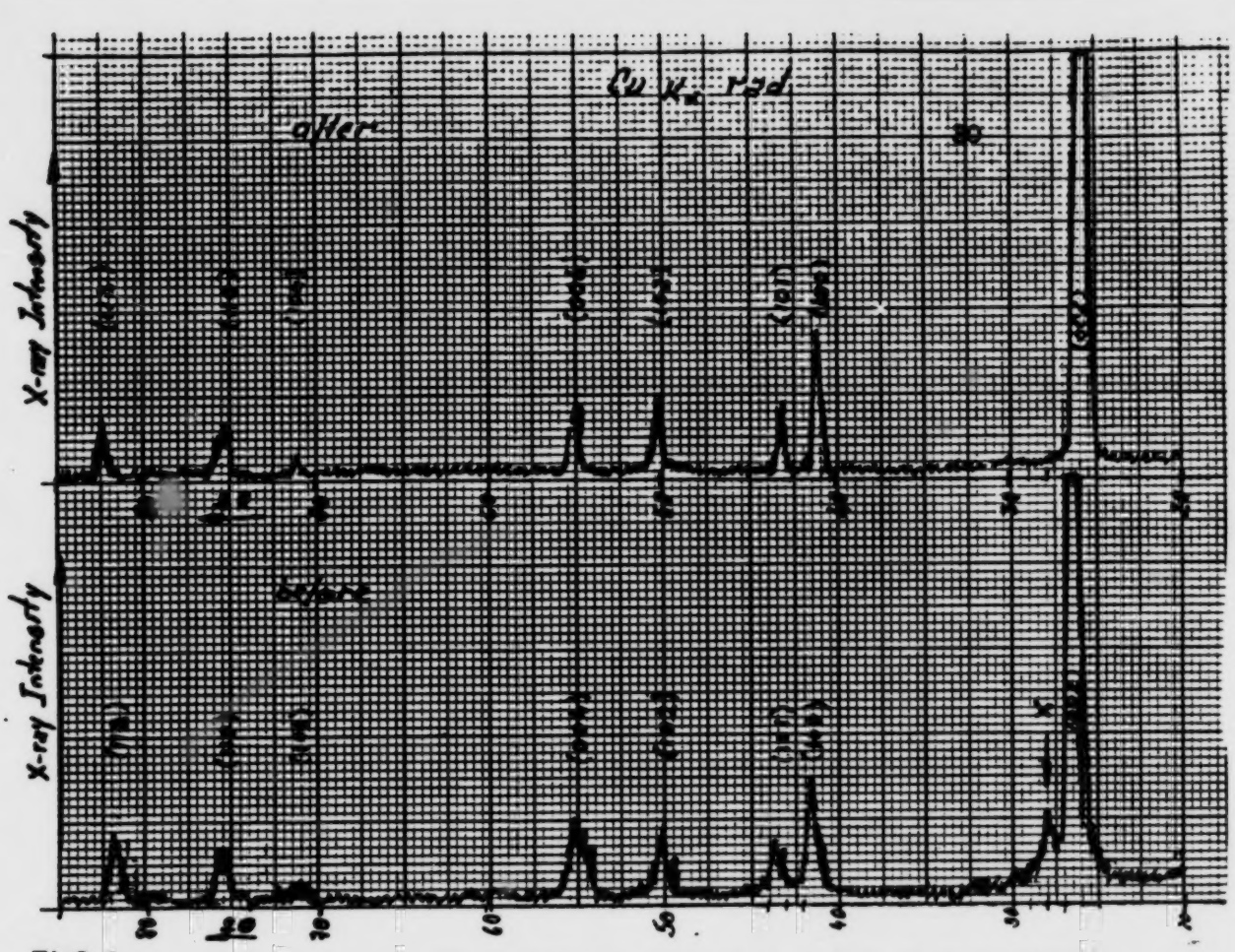

Fig3.4 X-ray diffractions on BN powder: a. before b. after heat treatment.

Fig.3.5a

Scanning electron image of BN heat-treated powder ×2,000

Fig.3.5 b. Secondary electron image (x5.000) -detail from a.

3.2 BORON NITRIDE FIBRE

The Electrofuel Manufacturing Company in collaboration with the Ontario Research Foundation developed a new low cost route to Boron Nitride fibre production. Boron nitride fibres, like carbon fibres, cannot be formed by conventional fibre forming techniques as the material decomposes before melting. This was the first ceramic product developed by Electrofuel and its manufacturing process has undergone quite a number of major changes over the intervening years. The main thrust has been in correlating production methodology with structural characteristics and fibre properties.

3.2.1 X-RAY DIFFRACTION ANALYSIS

Several papers have been published on the crystalline structure of BN fibers, but still several questions remain unanswered. Boron Nitride has a crystal structure similar to graphite but with a distinctive difference in the nature of layer packing. In hexagonal BN, the rings of atoms are packed directly on top of one another. The distance between layers is about 3.33 Å while the B-N bond distances within rings are 1.45 Å *. Another crystallographic form of BN, called turbostratic structure, has also been reported **. This turbostratic structure can be described as one consisting of two dimensional layers of hexagonal rings which are stacked at regular intervals; however, there is a complete lack of orientation from layer to layer. Turbostratic BN does not have a three dimensional lattice structure and the structure is thus distinguishable by the absence of multiple (hkl) reflection.

---

* R.S.Pease, Acta Cryst.,5.(1952).356

** G.Thomas, N.A.Weston, T.E.O'Connor,

X-ray analysis of BN fibers often results in diffraction patterns corresponding to turbostratic structure * , although there may be an inconsistency in interpreting fiber structure as turbostratic, since the properties differ considerably from those reported for turbostratic BN. The contradiction between structure and properties has been explained in terms of crystallite size and differences in the interlayer spacing ** . The crystal dimensions of turbostratic boron nitride fiber is in the range of 15.40 Å upto several thousand Å. The interlayer spacing approaches 3.33 Å which is close to that of the hexagonal phase. The only factor that distinguishes the "turbostratic" structure from hexagonal is the absence of any orientation in the c direction. Otherwise, the sizes and shapes of crystallites may be similar and, in fact, various forms may exist within the same grain.

X-ray diffraction shows that the crystalline structure of BN fibre strongly depends on the manufacturing process parameters. The structure of fibers can be changed from amorphous to highly crystalline (70%). X-ray diffraction patterns for fibers with different degrees of crystallization are shown below:

---

* G.Economy, R.Lin "Boron and Refractory Borides". Springer Verlag,(1967),552

** G.Economy, R.V.Anderson, V.I.Matkovich. Appl.Polymer Symp..9.(1969).377

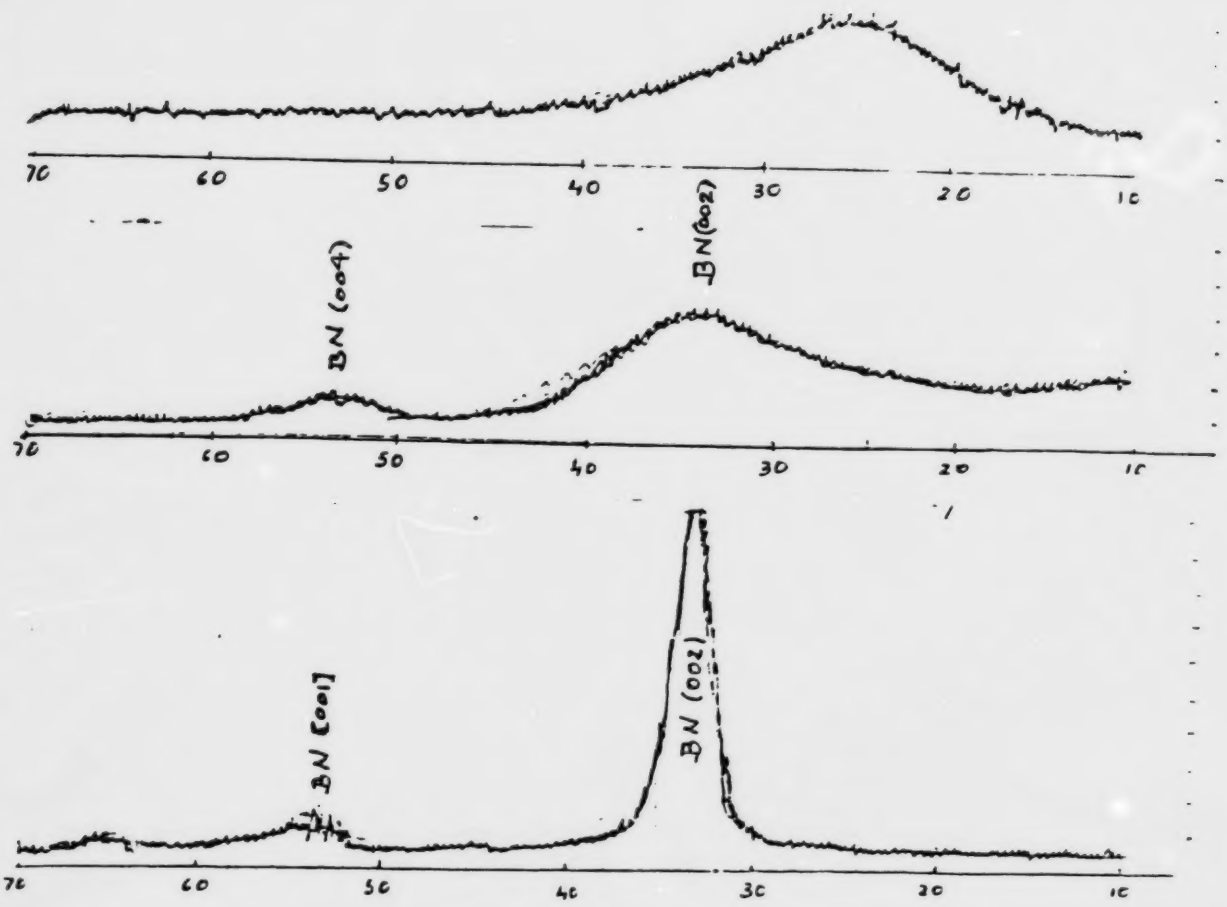

Fig.3.4 X-ray diffraction patterns of BN fibers obtained at different temperature, showing: (1)- amorphous, (2) -low and (3) -high crystallinity structure.

X-ray diffraction patterns were all recorded under the same

experimental conditions, using Cu k_{α} radiation with a Ni filter.

Sample (1) has a completely amorphous character and no crystalline order can be found. An amorphous structure for BN fibers has not previously been reported in the literature. The X-ray diffraction pattern of sample (2) showed an amorphous structure, but with local ordering in the "c" direction along the fibers: the two broadened peaks correspond to (002) and (004) reflections. The graphitization index for this sample, using the (002) diffraction line, was found to be 0.22. This locally ordered structure could be a turbostratic BN form mixed with small amounts of amorphous B-O-N. The third fiber sample has the highest degree of crystallinity with a preferential orientation of the unit cells "c" axis along the fiber. The (001) group of diffraction peaks are narrow and the variation of X-ray intensity can be described analytically. A locally ordered structure in the basal planes (perpendicular to the fibers) broadens the (h00) and (hk0) type reflections.

The presence of B_2O_3 in the fibers has not been seen by X-ray diffraction in any of the analyzed samples, in agreement with the expectation that any B_2O_3 present would be glassy and entirely amorphous.

In addition, X-ray diffraction analysis was performed for samples before and after heat-treatment (recrystallization). BN fibers were heat-treated in a vacuum furnace in a nitrogen atmosphere and at a temperature about 2000 degrees C. X-ray diffraction patterns of amorphous BN fibers before and after heat treatment are shown in Fig. 3.7.

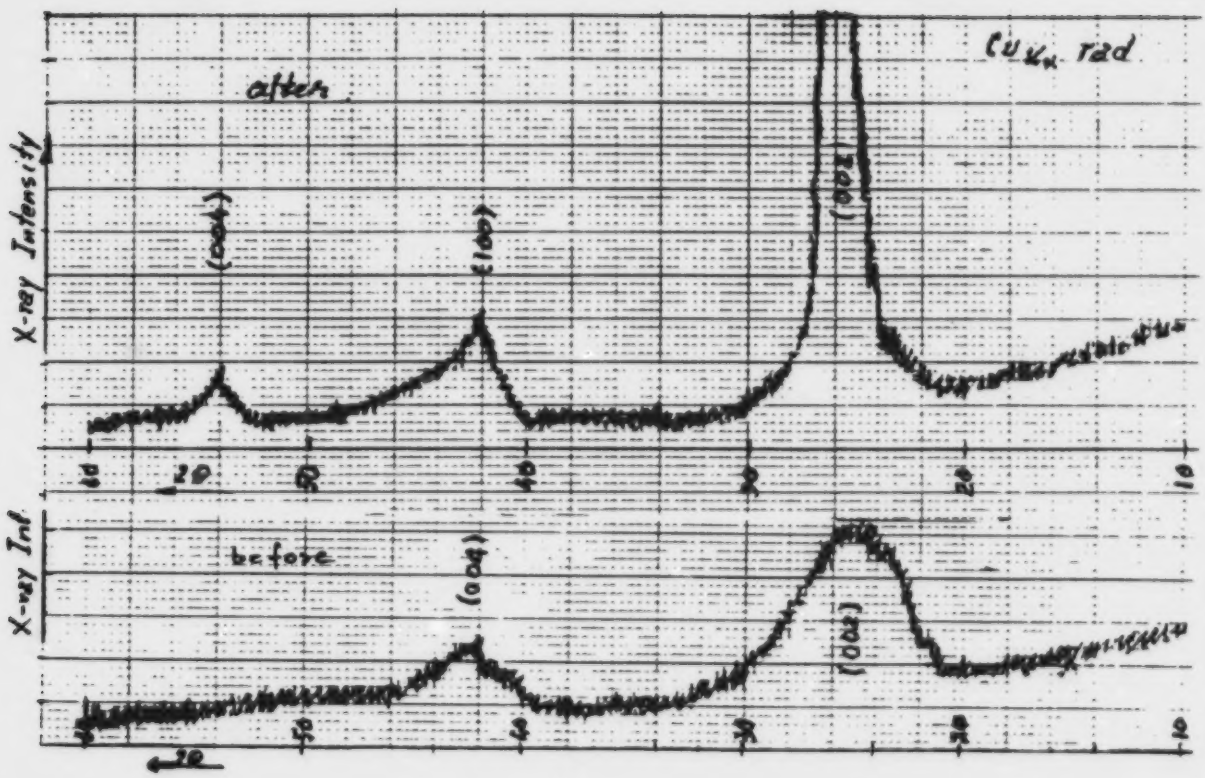

Fig.17 X-ray diffraction patterns of BN fibers before and after heat-treatment.

Structural modifications occur during the heat-treatment, the treated sample becoming more crystalline. The diffraction pattern shows a high degree of crystallinity similar to that observed for highly crystalline untreated BN fibers.

3.2.2 MICROSCOPY

Morphological studies of BN fibers using electron microscopy have been done in other laboratories. and the results correlated with crystallite size and B2O3 content*.

In fibers with diameters over 10 um, internal defects were noticed by SEM, while for less than 10 um no defects were detected.

Scanning electron microscopy was used at Electrofuel to study the fiber shape and to determine fiber diameters. No significant differences have been noticed between the scanning electron images of amorphous and crystalline BN fiber. Fig.3.8 is a secondary electron image of an amorphous BN fiber sample and Figs.3.9 and 3.10 are similar scanning images of crystalline fibers.

---

* J.Economy & R.Lin in " Boron and Refractory Borides "
V.I.Matcovitch (Ed), Springer-Verlay,1977

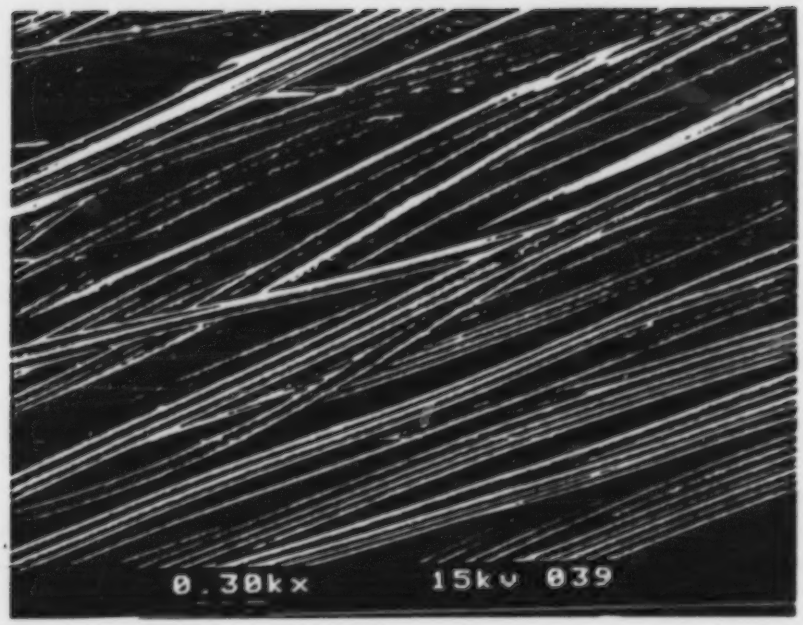

Fig.3.8 a. Scanning electron image of amorphous BN fibres

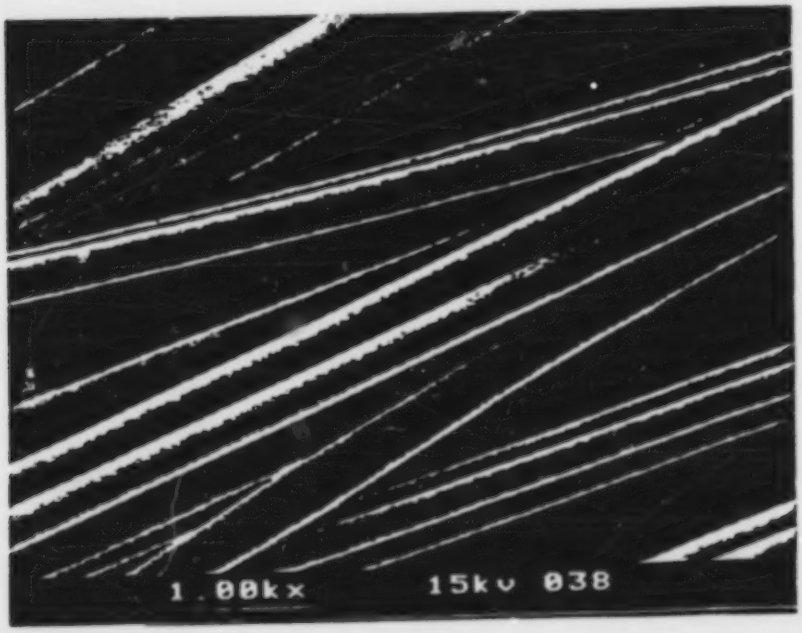

Fig.3.8 b. SEM image at higher magnification showing amorphous BN fibers

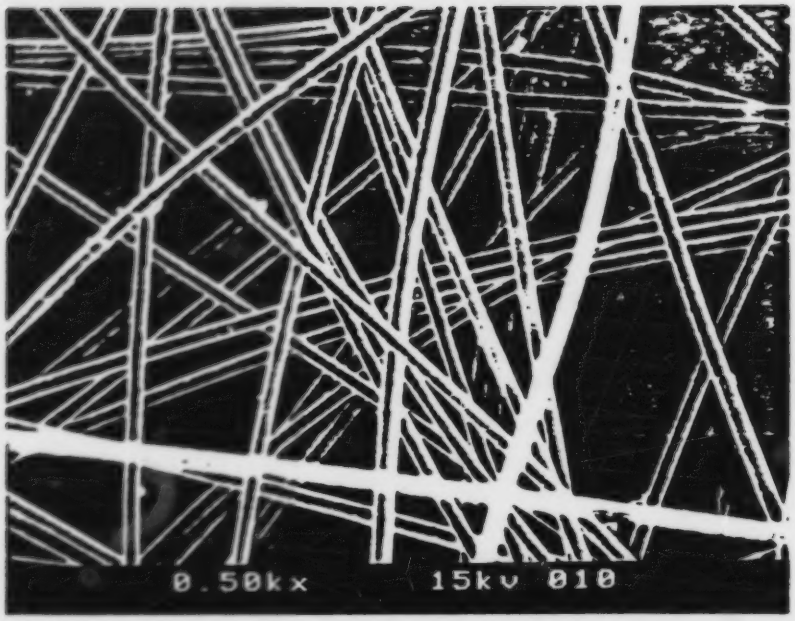

Fig.3.9 a. Secondary electron images of crystalline BN fibers

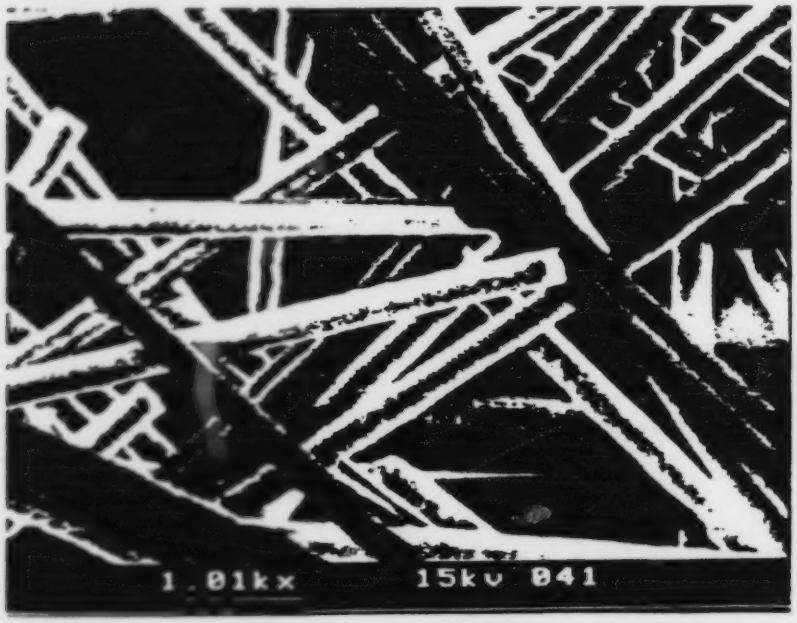

Fig.3.9 b. Detail from a. Crystalline BN fibers -higher magnification.

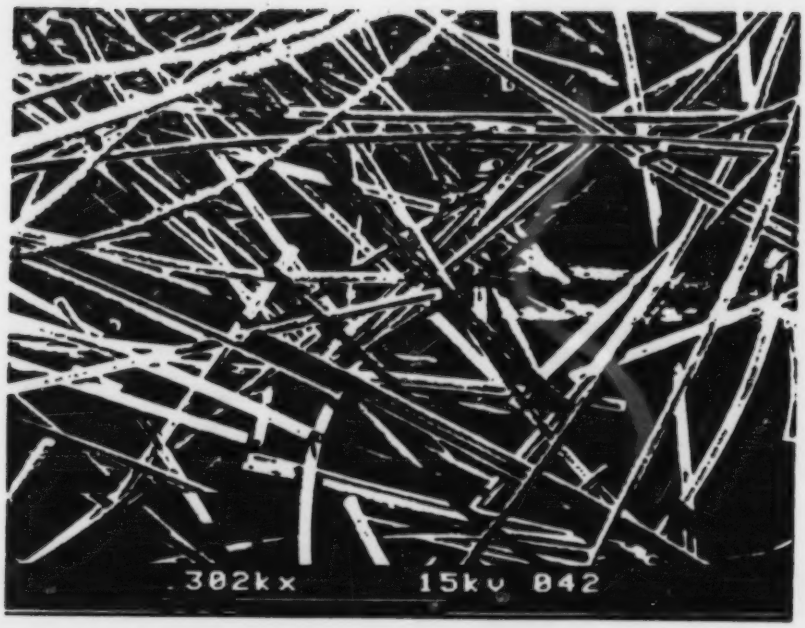

Fig.3.6a. Other SEM image of crystalline BN fibers

Fig 3.6b. Higher magnification showing some details.

The fibres have uniform thickness in the range of 3-5 μm for both samples. The surface is smooth in the case of amorphous BN fibers, (Fig.3.8 b) while some white spots can be noticed on the surface of the crystalline BN fibers (Fig.3.9 b.and 3.10 a.b).

3.2.3 B2O3 CONTENT

Like all boron nitride, boron nitride fibre oxidizes to B2O3 when exposed to oxygen at elevated temperatures. The following figure shows the oxidation of BN fibre in comparison with carbon fibre. It is largely the presence of the protective B2O3 glass that restricts oxidation below 900 degrees C. Fibres, by virtue of their

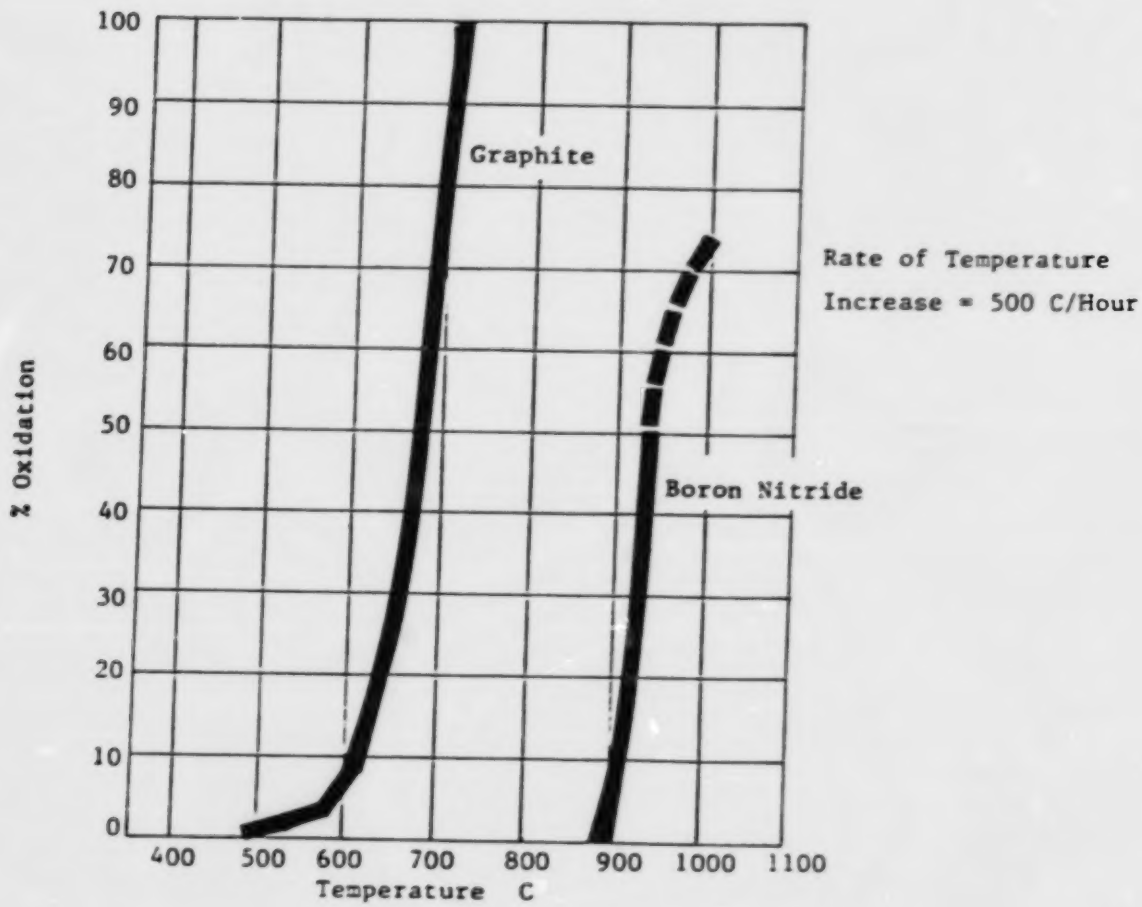

Temperature dependance of Oxidation.

manufacturing process, inherently contain less B2O3 than hot pressed BN. This is reflected in many properties, but a convenient example is the electrical property shown below.

Electrical Resistivity of Boron Nitride

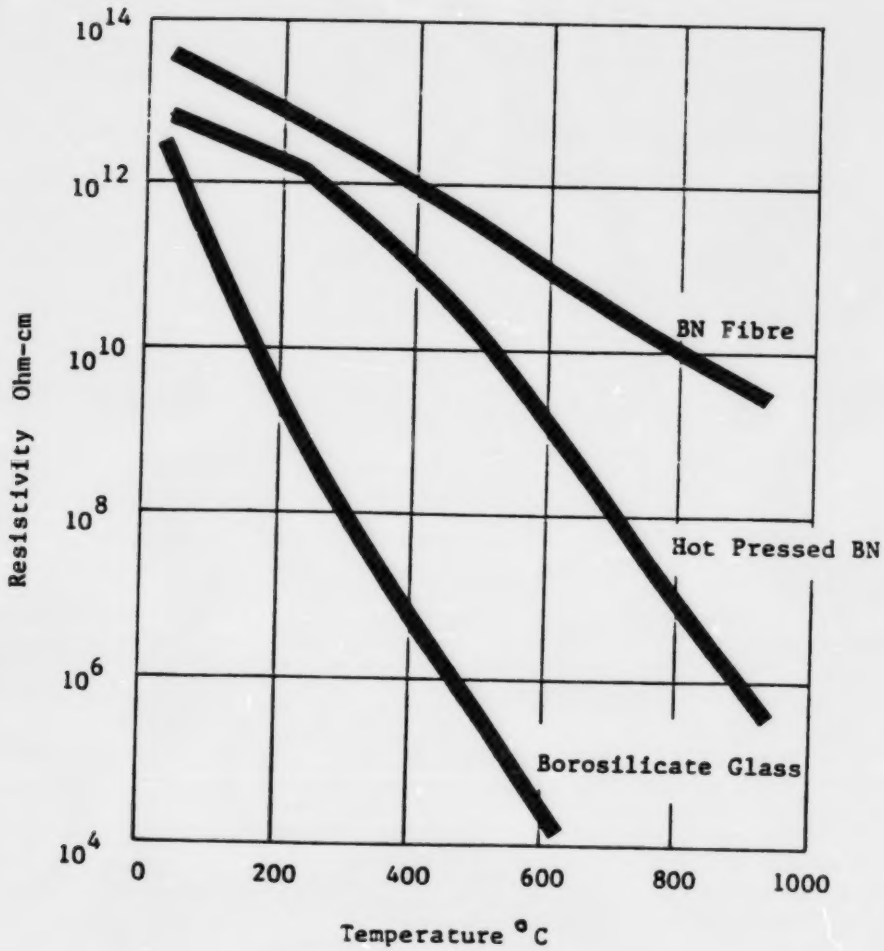

The residual conductivity of BN is mostly due to residual B2O3. The curve for borosilicate glass is for comparison only.

As in B2O3 powder (or solids), the B2O3 is measured by the acid soluble boron method. Depending on processing conditions, the B2O3 content of virgin fibre can be as high as 20%, but as low B2O3 content seems to correlate with improved fibre properties, the B2O3 content is now routinely kept below the 0.5% analytical detection [illegible] for quality control purposes.

3.3 OTHER POWDERS

3.3.1 TITANIUM DIBORIDE

Titanium diboride is used to give electrical conductivity to BN composites for use in heating elements, evaporator boats, etc. A number of manufacturers supply titanium diboride (TiB2) which they make under various conditions by carbothermic reduction of titanium dioxide and boric oxide. There are significant differences in powders from the various manufacturers and some characterization is in order.

X-ray diffraction, optical and scanning electron microscopy were used for structural characterization of starting TiB2 powders.

The scanning electron microscopy, by secondary electron emission, has shown big differences in the grain size distribution and particle shapes of TiB2 initial powders from Union Carbide and Advanced Refractory Technology. The Union Carbide TiB2 powder (Fig. 3.1 a and b.) has hexagonal particles in the range from 4 μm to 25 μm. The particles appear to be made by a direct chemical process rather than by grinding coarse bulk material. The particle size is quite fine with 50% less than 10 um and 90% less than 20 μm, as reported by the manufacturer.

On the other hand, the Advanced Refractory Technology (ART) powder appears to be ground from bulk material as can be seen from Figures 3.2 a and b. The ART powder has a wider grain size range (being estimated at 5 μm to 50 μm) and the particles have coarse and irregular shapes. Table 3.2 gives the particle size distribution and chemical analysis as reported by the manufacturer.

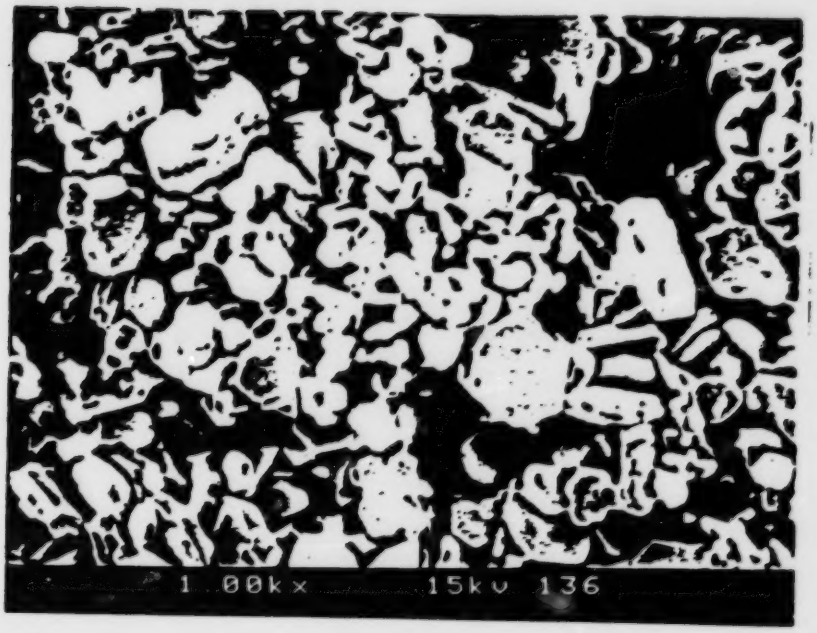

Figure 3.4 a. Scanning electron microscopy image of TiB2 powder (source U.C.)

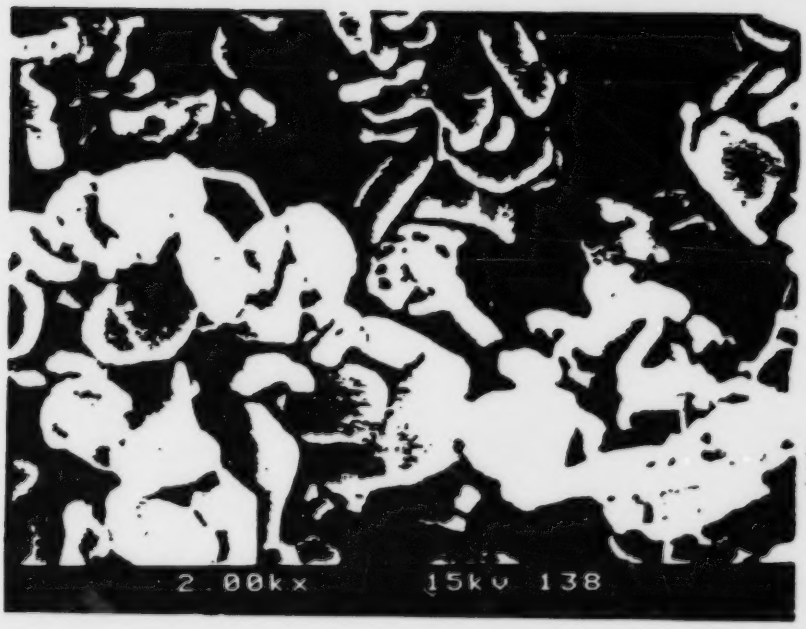

Figure 3.4b. Higher magnification for the same sample.

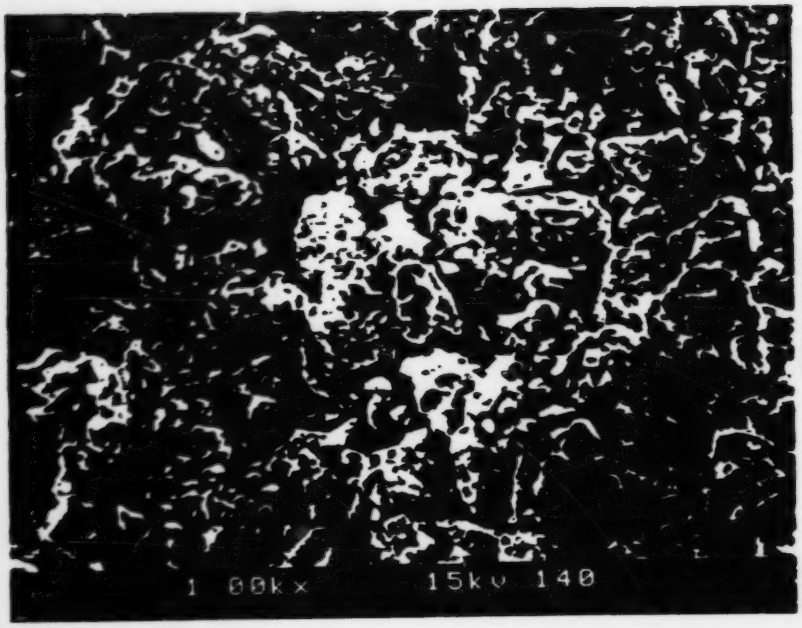

Figure 3.2a. Secondary electron image of TiB2 powder (source ART).

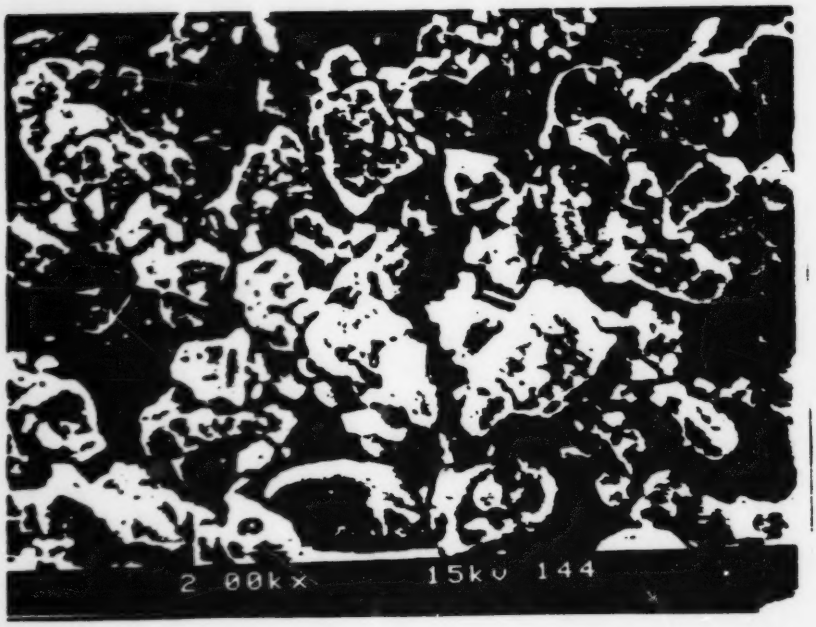

Figure 3. b. Detail from fig.2a at higher magnification.

Selected Physical Properties

Density, g/cm³: X-ray Method	4.25
Surface Area, m²/g	0.5 ± 0.1
Spherical Diameter Equivalent to Surface Area, μm:	2.8
Average Particle Size, μm: Fisher Subsieve Sizer	3.4
Microtrac	10.4 ± 1.0

Typical Particle Size Distribution (Microtrac Method)

% Weight Less Than Diameter	Diameter (μm)	% Weight Less Than Diameter	Diameter (μm)
10	4.8	75	15.5
30	7.9	90	19.7
50	10.6	100	44.0

Typical Screen Analysis

U.S. Mesh	% Retained	U.S. Mesh	% Retained
35	0.01	325	0.96
100	0.15	Balance	98.67
200	0.21		

Chemical Analysis (Wt%)

	Typical	Range
Ti	67.50	66.60 - 68.14
B	30.36	30.36 - 31.16
C	0.49	0.30 - 0.70
O	0.43	0.30 - 0.50
N	0.09	0.08 - 0.12
Fe	0.01	
Ti/B (Stoichiometric 2.216)	2.204	2.105 - 2.282

Cubic Phases by X-ray Diffraction (V/O) < 0.5 (as ratio of integrated intensity of cubic [200] diffraction peak near 2.16 Å to TiB_2 [101] and diffraction peak at 2.033 Å)

Trace Element Analysis (ppm)

Al	40	Cu	< 30	Ni	< 16	Se	< 16	Zn	< 9
Ca	< 10	K	< 30	P	60	Si	< 19	Zr	24
Co	16	Mo	< 16	Pb	< 24	Sn	< 15		
Cr	19	Na	< 30	Sb	< 50	W	< 16		

< not detectable by induction-coupled plasma emission spectroscopy at stated limit

UNION CARBIDE

ADVANCED REFRACTORY TECHNOLOGY

Composition:

Ti ⟶ 68.08%, B ⟶ 30.95%

O ⟶ 1.2%, C ⟶ 1.54%

Particle Size:

97% < 9.08 μm, 50% < 4.12 μm,

6% < 1.46 μm

TABLE 3.2

The X-ray diffraction pattern of ART starting TiB2 powder, recorded with Cu k_α radiation, shows a hexagonal structure, the lattice parameters being a = 3.028 Å and c = 3.228 Å.

In this respect the two powders are similar and thus differences in the properties of composites containing these powders will in most cases be related to particle shape and size distribution. Of some additional importance is chemical purity, and in particular carbon content. The carbothermic reduction process leaves behind carbon and carbides which are deleterious in some applications. It has been reported, for example, that traces of sodium from solution in molten aluminum can intercalate the residual carbon and result in rupture of the particles. Carbon analysis has not been carried out in our laboratory (distinction between carbon and carbides would also be informative), but manufacturers' data indicate considerable variability in this regard. For Union Carbide powder, reported carbon is about 0.5 %, while for ART it is about 1.2 %.

3.3.2 ALUMINUM NITRIDE

While process development leading to a full-scale manufacturing capability is currently underway at Electrofuel, powder is currently purchased from a number of manufactures. The particle sizes, x-ray diffraction patterns, etc., are evaluated at Electrofuel.

The area most actively addressed by all manufacturers is the oxygen content of the powder (always in the low percent levels). For BN composite applications in the presence of considerable B2O3, this is of little importance, while particle size is of greater significance.

4 PROCESSING

Effective processing, from powder preparation through firing, is the key to obtaining reproducible composite properties. Considerable trial-and-error is involved in this area, and where results are entirely empirical, only the successful procedures are reported.

4.1 POWDER PREPARATION

While boron nitride powder needs little initial preparation, the other powder additives do require some processing for agglomeration, de-agglomeration and particle sizing. Titanium diboride, especially ART powder, contains occasional lumps of several millimeters diameter which must be removed by coarse sieving. As there does not seem to be a continuity of coarse particle sizes, screening at 50 mesh seems to remove the entire coarse fraction. Agglomeration of the TiB2 into moderate strength agglomerates of about 100μm diameter assists further blending and improves densification, strength and conductivity properties of the composites. This might best be performed by spray drying, but at present the procedure used is to blend with PVA/water binder and screen (50 mesh) in the semi-dry condition. Thorough drying at slightly elevated temperature (130 degrees C) completes the procedure.

The other particles used in the present composites require de-agglomeration as they are received in a naturally agglomerated state and should be intimately mixed for best results. The most effective procedures have been ball milling for short periods and ultra-sonic dispersion. While ultra-sonic dispersion is rapid, ball milling has so far been easier to control. Re-agglomeration is not observed in ball milling.

4.2 BLENDING

A number of blending procedures have been tested for blending of the powders of composites. Dry blending, wet blending, high speed, low speed, etc. have been tested and in all cases the wet blending procedures have been most effective, especially those procedures involving the mix as a smooth but stiff paste. We believe that the effectiveness of wet mixing over dry mixing in all cases is due to the high electrical resistivity of dry BN powder. The powder tends to acquire a static charge which interferes with effective blending. This is noticeable in the way the powder segregates at the edges of the mixing chamber and in dead zones. It should be noted in this regard that the resistivity of BN is much greater than that of other insulating ceramic powders. High shear paste mixing does seem to be effective and good blends can be obtained with relatively short mixing times (1/2 hour or less) if the initial powder preparation has been carried out correctly.

After paste mixing the powder must be dried for cold pressing, this

drying being done in a large convection oven with good temperature control. Speed of drying is set so as to be complete in two four hour stages with mixing between stages. Bulk drying at this rate does not appear to cause significant segregation or oxidation.

4.3 COLD PRESSING

Boron nitride powder consists of fine platelike (flaky) particles which have very poor flow properties. In addition to the normal compaction problems in dry uniaxial pressing of fine powders, there is an additional problem of preferential orientation of BN flakes with high aspect ratio. Under uniaxial pressure, the flakes tend to orient such that their basal planes tend to be perpendicular to pressing direction. Pressing defects such as lamination and end-capping, which were observed when compacting virgin fine BN powders must also be controlled. These defects are also frequently observed during compaction of other ceramic powders.

A particularly troublesome type of failure observed when virgin BN powder was compacted was end-capping. End-capping is that problem whereby cracks starting in the upper corner of a compact move towards its center at a 10 degree-20 degree angle relative to the top surface. If the problem becomes severe enough, the top may break out of the pellet, resulting in a circular end cap of conical shape with a 140 degrees-160 degrees included angle, as shown in Figure 4.1. Thompson* has published a finite element computer analysis of end-capping in cylindrical compacts, which calculates the tensile stress buildup accompanying top ram withdrawal. As shown in Figure 4.2, the axial compressive punch pressure results in radial compressive die wall and hoop stresses which are not relieved fully when axial pressure is removed during decompression. As the load on the punches is released, the tablet will expand axially owing, initially, to its normal elastic recovery and,

*Thompson R.A., Am.Cer.Soc.Bull., 60(2), 1981, Part I, 237; Part II, 244; Part III, 248.

secondly, to the Poisson's ratio effect of the residual radial and hoop stresses in the compact. The net axial strain ε_a in this circumstance is given by

$$\varepsilon_a = \frac{\nu}{E}(\sigma_r + \sigma_\theta)$$

where σ_r and σ_θ are the radial and hoop compressive stresses in the compact, and ν and E are Poisson's ratio and Young's modulus for the material.

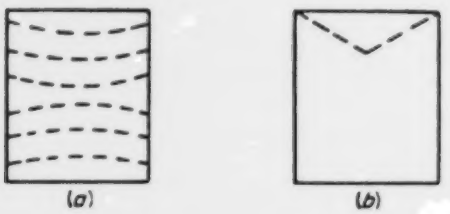

Figure 4.1 A schematic of typical compact defects observed when pressing virgin BN powder
a) end-capping, b) lamination

A ceramic compact tends to behave like a brittle material and it is often unable to accommodate this imposed strain by plastic flow, in which case tensile failure results. A further factor is the differential expansion of adjoining areas of the compact due to the non-uniform distribution of stress which occurs on compaction and which was highlighted by Train* This effect, illustrated in Figure 4.3, will also set up additional shear stresses in the compact.

* Train [1956] : F.Train, J.Phar.Pharmac. 8,745,1956

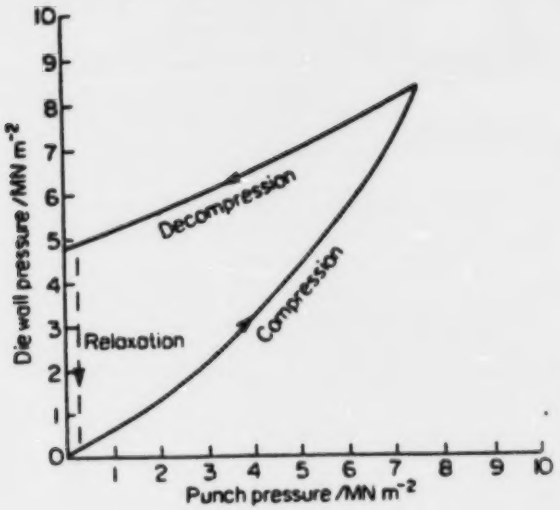

Figure 4.2 Axial and radial pressure cycle

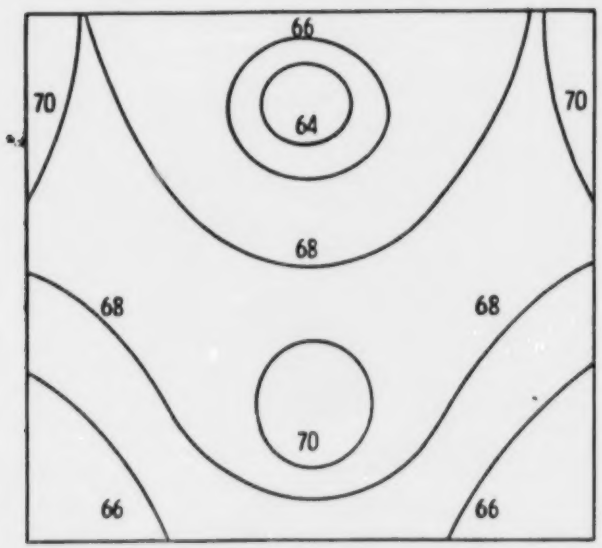

Figure 4.3 Apparent density distributions within a lubricated compact, expressed as percentage of solid present (from Train)

A third possibility is related to the dynamic situation. If the load on the punches is released quickly enough, tensile unloading waves will propagate from both punch tips and travel towards one another, relieving the elastic compressive stress in the compact as they pass. However, at the instant when they meet, the two pulses will add and there will be a net tensile stress on the tablet cross-section at that point equal in magnitude to the original elastic axial compressive stress. Thus as the tensile strength of a ceramic compact is very much less than the maximum applied pressure, under these circumstances tensile failure of the tablet in a plane perpendicular to the axis of the die is probable.Owing to the still porous nature of the compact. there will be no shortage of sites from which a crack could propagate.

The second stage of the cycle at which capping may occur is during ejection of the compact from the die. That part of the compact which is clear of the die will be free to recover elastically in the radial direction and also, to a certain extent, in the axial direction as die-wall friction may have previously prevented complete axial expansion. However, the lower part of the compact remaining in the die will still be confined and this differential strain distribution will lead to shear stresses being set up. If the original stress in the compact, particularly in the radial direction. is high enough,then this will cause fracture along the top of the compact causing it to 'cap'.

Hiestand and coworkers have extensively studied the effects of decompression for pharmaceutical systems and state that whether or not fracture occurs during the shear deformation which accompanies decompression depends on the ability of the material to relieve the stresses by plastic deformation without undergoing brittle fracture, and this ability is a time-dependent phenomenon. Those materials that relieve stresses rapidly are less likely to 'cap' or laminate.

From finite element analysis. Thompson demonstrated that as the holddown pressure PH is reduced to zero (see Figure 4.4), a crack would initiate from the upper corner of the compact at about 10 degrees-20 degrees angle as practically observed in many systems. He also deduced the effect of various process parameters on end-capping, and his conclusions are summarized in Table 4.1.

Significant parameter	Effect on end-capping
η, powder fluidity index	Increased η is bad
γ, powder/die-wall coeff. of friction	Increased γ is bad
L/D, length-to-diameter ratio	Increased L/D is bad
PH, holddown pressure	Increased PH is good
ε_{max}, green tensile strength	Increased ε_{max} is good

Pa, the pressing pressure, also affects end-capping but in a more complicated way.

Table 4.1

It can be seen from the Table that increasing powder fluidity index (η) makes the problem worse. However, decreasing the powder fluidity has an adverse affect on the density gradients within the compact as shown in Figure 4.3, and hence is not a viable practical solution. The second parameter, powder/die-wall coefficient of friction (γ) must be reduced to prevent end-capping, and can be effected by judicious choice of lubricant and good surface finish on mold walls.

The end-capping problem and the density variation within the compact limits the L/D ratio in uniaxial dry pressing. However, going from single-acting to double acting pressing essentially reduces L/D by a factor of 2, thus allowing twice longer compacts to be successfully pressed.

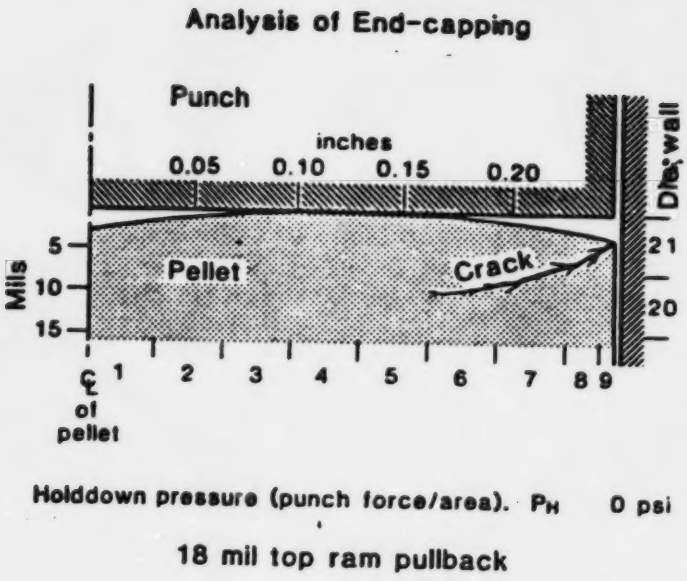

Figure 4.4 Finite element analysis of end capping

Holddown pressure (PH).i.e. the pressure maintained on the compact during ejection. is an effective method to reduce end capping of the compact. Cracking can normally be prevented when the holddown pressure is 25% to 35% of the compaction pressure.

Green tensile strength (σ_{max}) is normally a material property which normally cannot be significantly altered in pure powders. However, with proper choice of binder it can be engineered to prevent cracking.

Finally, right amount of taper on the mold helps in gradual release of radial stress during ejection and reduces the chances of end-capping and lamination. All the factors given above were studied on BN compacts and the design of the cold press mold on the 1.000 tonne press at Electrofuel has been optimized to prevent these compaction defects.

Figure 4.5 shows schematically the forces induced in a cylindrical compact being compressed from one end. If the materials being compressed were a perfect fluid, force would be transmitted isostatically and

$$FA = FL = FR$$

In a particulate system, however, friction is generated at the material-die wall interface as a result of induced radial force FR. Radial force FR is a function of the Poisson's ratio, ν, of the material and is related to force FA by the expression

$$FR = \frac{\nu}{1-\nu} FA$$

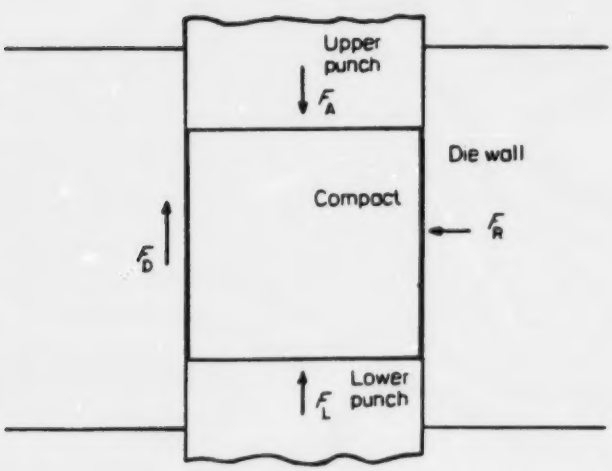

Figure 4.5 Forces operating on a powder under compression

A proportion of the applied force is transmitted to the die body and appears as die wall reaction force, FD. The remainder of the applied force is transmitted through the powder to the lower punch where it is measured as transmitted force, FL. The force balance may be expressed as

$$FA = FL + FD$$

If FD is considered as losses due to friction and FL as force available for densificaton. the FD incorporates losses due to both die wall friction. fw and interparticle friction. fI. Interparticle friction would be dominant at an early particle rearrangement stage of densification and die wall friction for the rest of the process. Each component may be expressed in terms of radial force, FR. Where w is the coefficient of die wall friction and I is the coefficient of interparticle friction

$$FD = (fw + fI) = FR\ w + FR\ I = FR(\ w +\ I)$$

and the force balance may be rewritten

$$FA = FL + FR(\ w +\ I)$$

Train measured in detail the distribution of pressure and corresponding variation in density in magnesium carbonate powder compacts. His results are shown in Figure 4.6.

His measurements revealed that for single ended compaction,the density was at a maximum at the outer circumference of the compact adiacent to the moving punch and at a minimum at the outer circumference adiacent to the stationary punch. More significantly, they showed that, while mean density decreased with increasing distance from the moving punch, a dense core of material existed on the compact axis near the stationary punch which was in many cases denser than material directly between it and the moving punch.

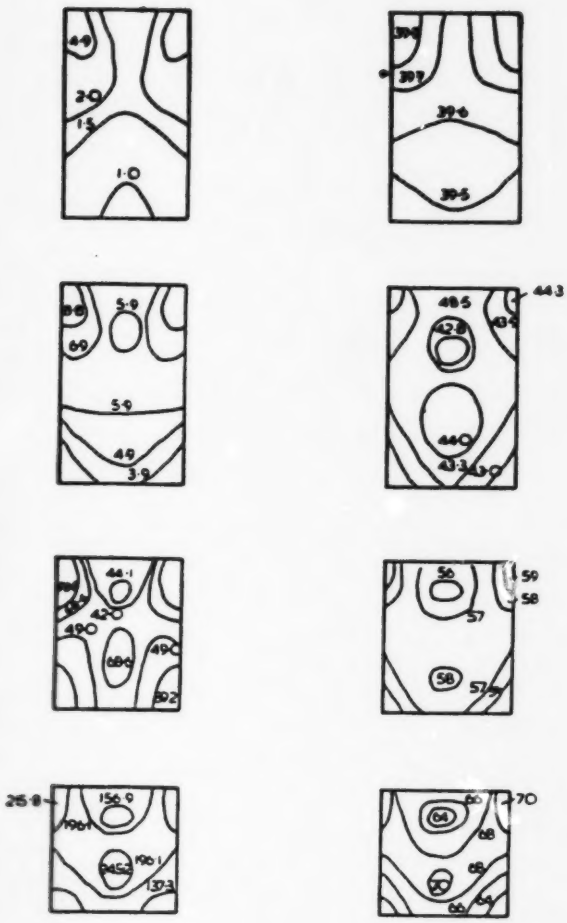

Figure 4.6 Relationship between observed pressure distribution (on left) and relative density distribution (on right) in compacts. From top to bottom, PA is 2.79, 8.83, 65.8, and 200.0 MN m-2 respectively (after Train)

Seelig and Wulf* attributed the phenomenon of non-uniform density distribution to die wall friction and demonstrated that lubrication of the die wall was effective in reducing it. Train supported their suggestion and proposed that capping and lamination faults in compacts were caused by non-uniform stress patterns generated. He proposed a simple explanation for the observed patterns of density

* Seelig,R.P. and Wulf, J,Trans. AIME, 171,516 (1964)

distribution based on the development of high density wedges of material owing to high shearing forces at the die wall adjacent to the moving punch. Figure 4.7 represents the forces developed in the compact. At equilibrium conditions the axial force is supported by the punch in the direction a and by the powder mass in direction b. The radial force component is supported by the die wall in direction c and by the powder mass in direction d. The resultant force acting on the powder mass is represented by k and because of axial symmetry in the compact the pressure front may be considered as a conical surface with focal point B. Area B will show enhanced pressure and density values compared with its surroundings because of effective pressure concentration. The wedge shaped area adjacent to the moving punch, bounded by dotted lines will be subject to high shearing forces and will be highly densified. The central area A on the axis will be subjected to negligible shearing forces and will be partially protected from axial normal pressures by the vaulting effect of the high density wedges. Area C adjacent to the stationary punch will undergo no movement relative to the die wall so shearing forces will be absent. Density will be low since consolidation will depend on transmitted axial forces only.

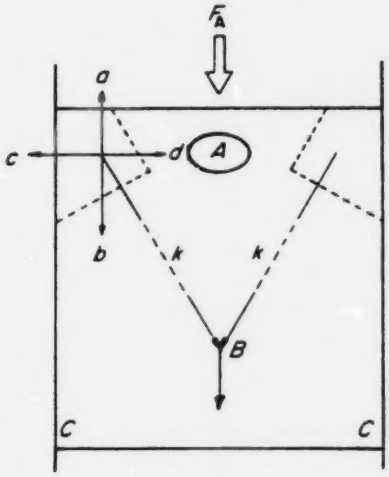

Figure 4.7 Development of pressure pattern (after Train)

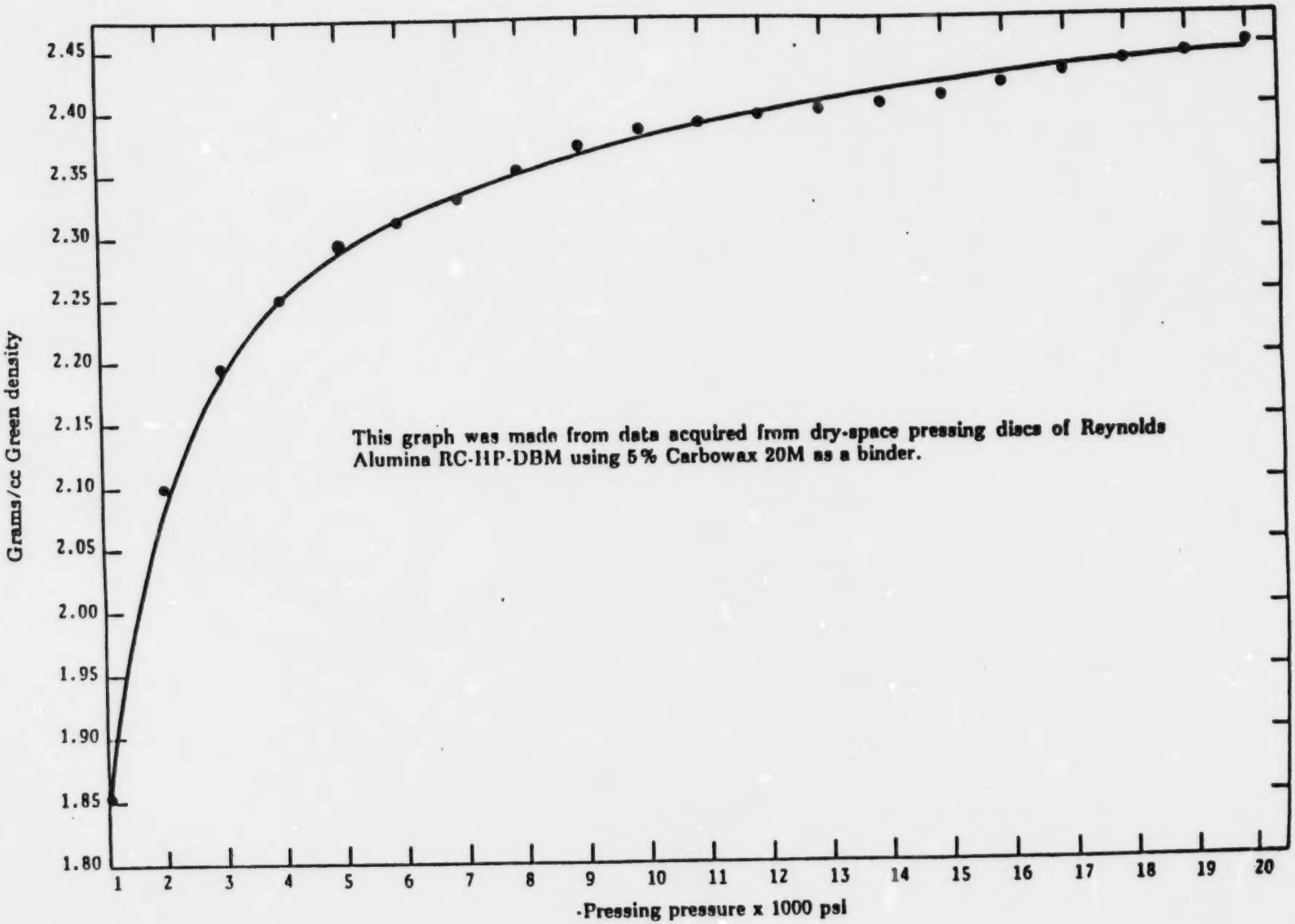
Grams/cc Green density
2.45
2.40
2.35
2.30
2.25
2.20
2.15
2.10
2.05
2.00
1.95
1.90
1.85
1.80
1 2 3 4 5 6 7 8 9 10 11 12 13 14 15 16 17 18 19 20
Pressing pressure x 1000 psi
This graph was made from data acquired from dry-space pressing discs of Reynolds Alumina RC-HP-DBM using 5% Carbowax 20M as a binder.

When pressing powders, initially there is a rapid increase in density of the compact as the pressure is increased and then it reaches a plateau as can be seen from Figure 4.8 for fine alumina. A number of stages have been identified in the densification process (shown by breaks in the Density - log Pressure plots). which can be summarized as:

1. Particle or granule rearrangement which takes place at low pressures (< 200 psi). Densification at this stage is increased significantly by vibration. Punch travel in this stage ranges between 25% to 50% of total, depending on the porosity of the feed material.

2. Granule deformation (100 to 10,000 psi) when coarse interstices are eliminated by granule deformation.

3. Granule fracture which occurs simultaneously with deformation process and leads to rapid filling of interstices between granules.

4. Bulk compression of the material itself (> 10.000 psi).

Densification during Stage 2 and 3 typically exhibits a linear relationship between relative density and log pressure. followed by a second linear dependence of density on log pressure but of greater slope, as can be seen from Figure 4.9. The critical stress corresponding to the change in slope (known as "breakpoint pressure") is interpreted as a qualitative index of the fracture stress of the granules leading to continued sliding and rearrangement. The compaction slopes for applied pressures exceeding the "breakpoint pressure" are similar for specimens of the same material with different powder character, whereas the initial compaction density is very sensitive to the powder character.

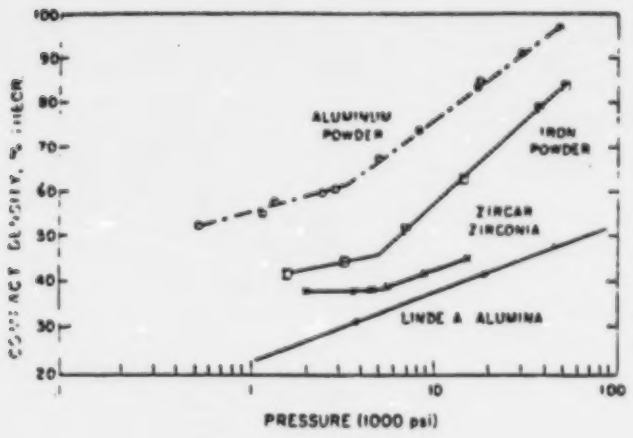

Figure 4.9 Variation of relative compact density with log pressure

Thus, strength of granules or agglomerates are of great significance. Fine powders require agglomeration to improve their flow properties; however, this agglomerated structure must be broken down during cold pressing, so as not to result in entrapped porosities within "hard" agglomerates which will result in flaws in the final sintered material. Thus, the binder system must be properly engineered to give "soft" agglomerates which crush during cold pressing.

In order to provide a free flowing, dust free feed to the compaction process to ensure uniform die filling and uniform compaction behaviour, the fine powder must be granulated. Two different approaches are possible. One choice is by the addition of a binder when, as already indicated, the material compression characteristics may be altered to minimize pressing faults such as capping and lamination. The binder also acts as a lubricant both internally and at the die wall, improving pressure transmission and reducing die wall frictional effects. The choice of binder is based on good melting behaviour, compatibility with the powder, ease of

removal and strength of agglomerate obtained. In the case of TiB2-BN composites. PVA was used as a binder.

However, in the case of pure BN no binder was used as high purity of the product is required. Instead. a technique known as "preslugging" was used.This consists of pre-pressing the raw powder into a convenient compact shape and crushing the compacts through screens to form granules of the required size. The preslugging pressure must be less than the applied pressure for the final die compression by about an order of magnitude. Figure 4.10 shows the effect of preslugging alumina powder. As can be seen from the figure, significant improvement in density is demonstrated by this technique.

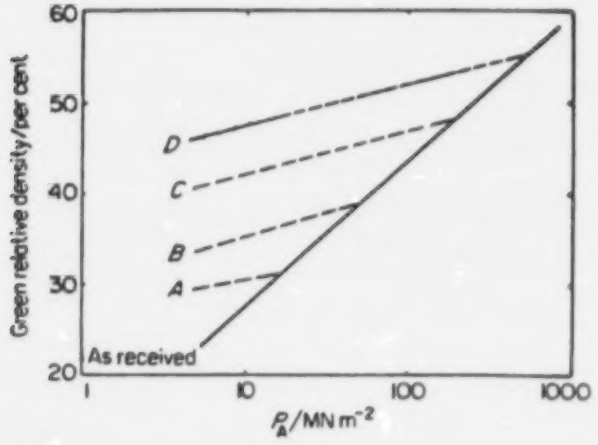

Figure 4.10 Increase in green density of alumina obtained by preslugging. The full line represents the alumina as received, and the broken lines refer to preslugging pressures A. 6.9: B. 27.6: C. 110.3; D, 441.3 MN m-2

More significantly, for BN this technique improved the tendency of BN flakes to align perpendicularly to the direction of pressing. This is important to reduce the anisotropy in the final hot pressed product which can lead to severe cracking and even disintegration due to large thermal expansion mismatch in 'c' and 'a' directions.

4.4 HOT PRESSING

The preparation of boron nitride remained a laboratory curiosity until the mid-twentieth century when hot-pressing techniques were devised permitting commercial development of hot-pressed solid boron nitride material. Boron nitride is a highly covalent material with a melting point of about 3000degrees C, and hence it is not amenable to pressureless sintering at even 2100 degreesC. Solid boron nitride with densities above 90% can only be manufactured by uniaxial hot-pressing (HP) or by hot isostatic pressing (HIP) processes. Each method has its advantages and disadvantages; however, in commercial practice, the lion's share of BN production worldwide is by hot pressing.

Hot pressing equipment is schematically shown in Figure 4.11. It consists of a mold, usually graphite, in which the ceramic powder is heated up with simultaneous application of uniaxial pressure through two punches (usually also graphite). This simultaneous application of temperature and pressure allows sintering of difficult to sinter covalent materials. Fiber (or whisker) matrix composite materials, difficult to sinter to full density without pressure are often effectively sintered by hot pressing.

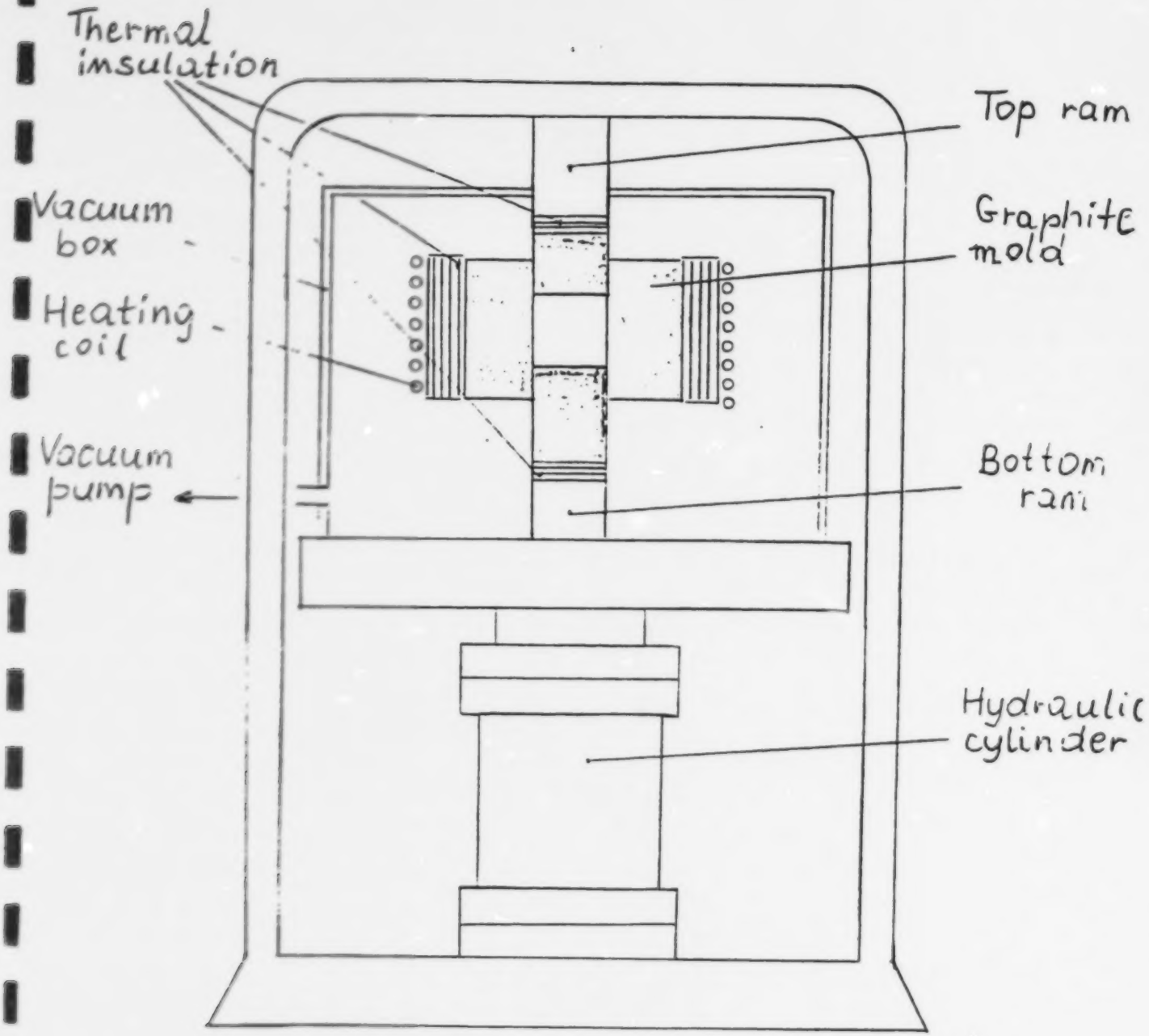

FIG. 4.11 HOT PRESS EQUIPMENT.

4.4.1 MOLD DESIGN

The mold can be either resistance heated or induction heated with the graphite mold itself acting as susceptor. Normally, hot pressing is carried out in vacuum or inert atmosphere. Pressures required are normally in the range of 2,000 to 15,000 psi with some fraction of this axial pressure being transmitted radially to the mold wall. There are some reports in the literature on continuous hot pressing processes and on multiple-layer multiple-cavity pressings. Toshiba is reported to have installed a production unit incorporating a carousel mold feed for continual automatic mold loading and unloading.

The maximum part size that can be hot pressed is essentially limited by the strength and size of available graphite mold material. Currently, parts upto 24 inches in diameter are commercially manufactured. Uniaxial hot pressing is normally limited to simple shapes.

The prototype hot press developed at Electrofuel is shown in Figure 4.11 It is a 300 ton press,capable of operating upto 2200 degrees C.

The design of hot-pressing molds is not trivial or straight forward as a number of parameters are not well defined. Table 4.3 lists a number of hot pressing die material that have been used or proposed for pressing

various materials.Refractory metals (W,Mo) and alloy (Ti-Zr-Mo, Ti-Zr-Mo-C etc.) molds are easily oxidized and are limited to medium temperature range of 1100°C to 1500°C by creep or stress-rupture behaviour. High cost and great difficulty in machining represent additional limitations. Refractory carbides such as SiC, TaC, WC, TiC and borides, such as TiB2 have been tried as hot pressing dies on a limited scale, the primary limiting factor being expensive machining costs. Oxide dies, especially high purity high density alumina has shown some promise, provided extreme care is exercised in loading and alignment. Both alumina and stabilized zirconia are limited by low thermal shock resistance, creep at elevated temperatures and machining costs.

UNIAXIAL HOT-PRESSING DIE MATERIALS

Die Material	Maximum-Use Temperature (°C)	Maximum-Use Pressure (p.s.i.)	Limitations[a]
Graphite	2500	10,000	Inert atmosphere usually required
SiC	1500	30,000	Reactive with many materials (DTM)
TaC	1700	8,000	Expensive (DTM)
WC, TiC	1400	10,000	Same as other carbides
TiB_2	1400	15,000	Same as the carbides
W	1500	3,500	Easily oxidized; creep limited
Mo	1100	3,000	Same as W
Mo alloys (TZM; TZC)[b]	1350	10,000	Same as W
Al_2O_3	1200	25,000	Extreme care needed in loading and alignment; limited thermal resistance (DTM)
ZrO_2	1180	5,000	Same as Al_2O_3
BeO	1300	10,000	Same as Al_2O_3
Inconel X,[c] Hastelloy,[d] Rene 41,[d] stainless steels	1100	10,000	Creep limited

[a] In this column, DTM is used to indicate "difficult to machine."
[b] Products of Climax Molybdenum Co.
[c] Product of The International Nickel Co.
[d] Product of Union Carbide Corp.
[e] Product of General Electric Co.

Table 7. Uniaxial Hot-Pressing Die Materials

Graphite has been widely used as hot pressing die and plunger material due to its high temperature capabilities (upto 2500 degrees C,its strength increases with temperature). low thermal expansion. ease of machining and low cost. A variety of graphite materials are available in extruded and molded forms. with densities varying from 1.4 to 2.0 g/cm3 and maximum grain size between 0.0004 to o.25 inch.

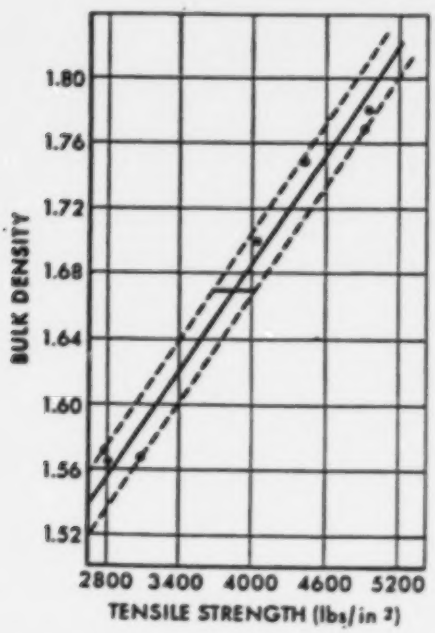

Figure 5.12 Bulk density (at room temperature) vs. tensile strength (at 1200OC) for EGP graphite

Figure 5.12 shows that room temperature tensile strength of graphite like that of most ceramic materials is strongly density dependent; it almost doubles as the density increases from 1.5 to 1.8 g/cm3 (for the same grain size). At the same density, with decreasing grain size, the strength generally improves, and so do machining tolerances and surface finish. (TABLE 9.1).

TYPICAL AVERAGE PROPERTIES (ROOM TEMPERATURE)

Grade	Cross Section Size (mm)		Max. Grain Size (mm)	Bulk Density (Mg/m^3)	Flexural Strength With Grain (k Pa)	Resistivity With Grain (microhm – metre)	Ash %
	Rounds (Dia.)	Rects. (Thk.)					
AGSR	5 – 32		0.20	1.58	17900	8.5	0.15
	38 – 70		0.41	1.58	19900	7.5	0.15
	75 – 145		0.76	1.60	13400	9.5	1.60
		25 – 145	0.76	1.60	13800	8.5	1.60
	150 – 130		1.5	1.60	11900	9.5	1.60
		150 – 610	1.5	1.60	10300	10.0	1.60
	255 – 305		3.0	1.60	10300	9.0	1.60
	355 – 610		6.4	1.60	7200	9.0	1.60
AGSX	25 – 70		0.41	1.69	26900	7.5	0.15
	75 – 145		0.76	1.70	17800	9.0	1.60
		25 – 145	1.5	1.70	18000	8.0	1.60
	150 – 230		1.5	1.70	17000	8.5	1.60
		150 – 610	1.5	1.70	16000	8.0	1.60
	255 – 305		3.0	1.68	12500	6.0	1.60
	355 – 890		6.4	1.67	9800	6.0	1.60
CS	76 – 254		0.76	1.66	18700	8.1	0.13
	305 – 610		0.76	1.73	15900	8.1	1.2
		381	0.76	1.72	15900	9.9	1.2
		441	0.76	1.62	15900	9.9	1.2
		508	0.76	1.74	15100	8.6	1.5
CBY	76 – 254		0.76	1.56	12300	9.0	0.2
	305 – 610		0.76	1.60	12300	8.5	1.2
		441	0.76	1.62	14200	8.3	1.2
CMX	762		1.5	1.72	9900	8.6	1.5
PGX	914 – 1854 *		0.76	1.75	13100	12.3	0.44
ECV	6 – 32		0.20	1.68	15900	8.2	0.005
	38 – 51		0.41	1.68	19300	8.2	0.005
ECL	76 – 254		0.76	1.68	18600	7.8	0.005
	305 – 457		0.76	1.68	18600	7.8	0.005
ATJ	All Sizes *		0.15	1.74	31600	11.3	0.12
CGW	All Sizes *		0.15	1.82	36600	10.4	0.13
EBP	All Sizes *		0.15	1.68	31600	11.3	0.005
EBX	All Sizes *		0.15	1.68	31600	11.3	0.018
CMG	All Sizes *		0.15	1.80	40000	10.0	0.6
CMGA	All Sizes *		0.15	1.80	40000	10.0	0.6

* Items formed by moulding, all others extruded

TABLE 4.4 . GRAPHITE GRADES

For hot pressing mold and ram applications fine grain molded graphite such as Union Carbide grade ATJ is normally reccommended. This material has tensile strength (R.T.) around 2800 psi and flexural strength (R.T.) around 4800 psi. However, they are limited to a size of 17 inches in diameter. On the other hand, extruded graphite with medium grain size, reasonably high densities (~1.74 g/cm3) and reasonable flexural strength (2800 psi) can be obtained upto 40 inches in diameter. An important property of graphite is that its strength increases substantially with increasing temperature as illustrated in Figure 4.13 . It can be seen that at 2000 degrees C the strength of graphite is 50% more than its room temperature strength. This fact can be used to apply a programmed (increasing) level of pressure with increasing temperature.

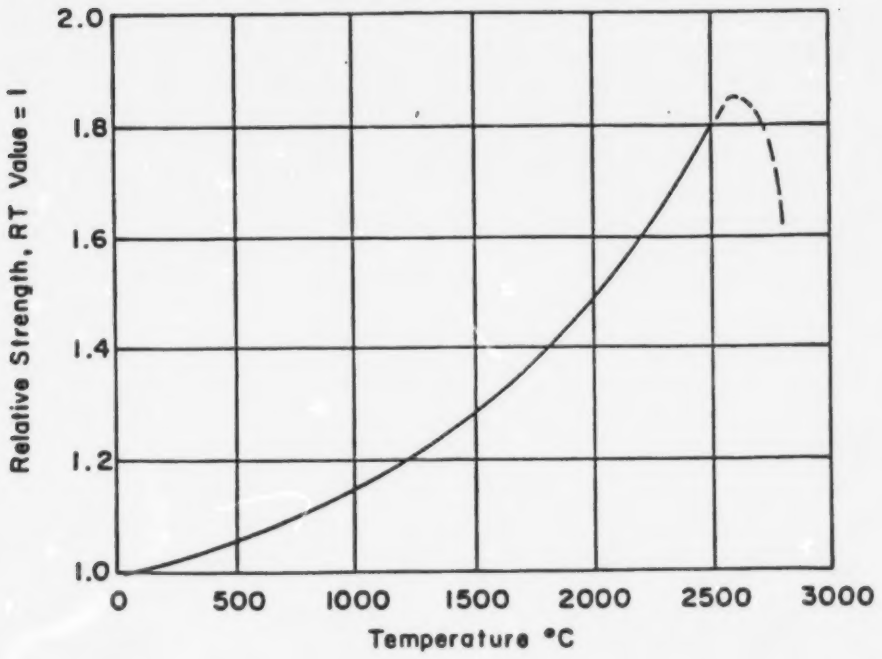

Figure 4.13 Typical effect of temperature on the strength of graphite

As the wall thickness of hot press molds normally exceeds the radius of the cavity, the mechanical behaviour is predicted using thick cylinder analysis in which the hoop and radial stresses vary along the wall as shown in Figure 4.14. The hoop stress at any radius r can then be shown to be

$$\sigma_H = \frac{P r_i^2}{r_e^2 - r_i^2}\left(1 - \frac{r_e^2}{r^2}\right)$$

where P is the internal pressure and, r_i and r_e are the internal and external radii, respectively. The maximum tensile (hoop) stress occurs at the inner wall and is given by

$$\sigma_{H_0} = P\left(\frac{1+R^2}{1-R^2}\right) \qquad \text{where } R = \frac{r_i}{r_e}$$

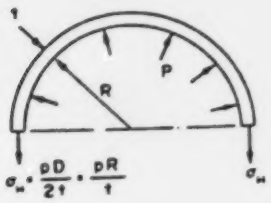

Fig. 10.1. Thin cylinder subjected to internal pressure.

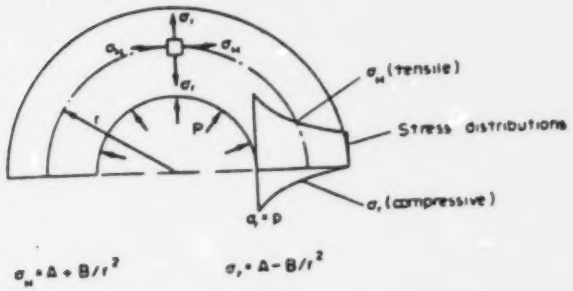

Figure 4.14 Thick cylinder subjected to internal pressure

Using such a stress analysis and conservatively estimated die wall loadings, a mold can be sized and its performance predicted to a certain extent. Deviations from predicted behaviour should be accommodated with conservative safety margins. From the perspective of safety margins, however, the situation is not a happy one. Pressing process requirements demand high pressures while the strength of graphite is limited. In addition, graphite availability in large sizes, and the diminishing effectiveness of increasing the outer diameter, limit the extent to which the mold can be strengthened.

Graphite is a brittle material. Strength measurements on brittle materials show a high variability and a dependence on the physical size and type of the test sample. This can result in serious errors when conventional design methods are used and strength values from a limited number of tensile tests are used in conjunction with stress analysis to predict failures in components subject to complex stress states. For example, the method of selecting a "safe working stress" that is some fraction of the yield stress, which is adequate for metal structures, cannot be applied to brittle materials with a statistical spread in strength values, because there will be a finite probability of failure for any applied stress above zero. Similarly, it may not be sufficient to predict a failure probability based on the mean fracture stress and standard deviation for a few tensile tests, because the implicit assumptions that the strength values are distributed normally and the fracture stress is independent of sample volume and stress state are not justified.

One design approach for brittle materials is to use the Weibull statistical theory of strength, in which the strength of a body under a tensile stress is assumed to be controlled by the distribution of surface or internal flaws. This theory has the potential for predicting failure probabilities in structures of any volume and stress state, including multi-axial stresses and stresses which are a function of position.

For graphite, strength values derived from tensile tests, bend tests, tube-burst tests, etc., show significant differences. Graphite behaves differently under uniaxial, biaxial and triaxial stress mode, which makes prediction of a component life under complex stress mode difficult from an uniaxial tensile or bend test results.

Figure 4.15 shows the results on internal pressure burst tests and diametral tests on ring specimens of graphite. It can be seen that none of the test results agree with the tensile or the 3-point bend strength of the material.

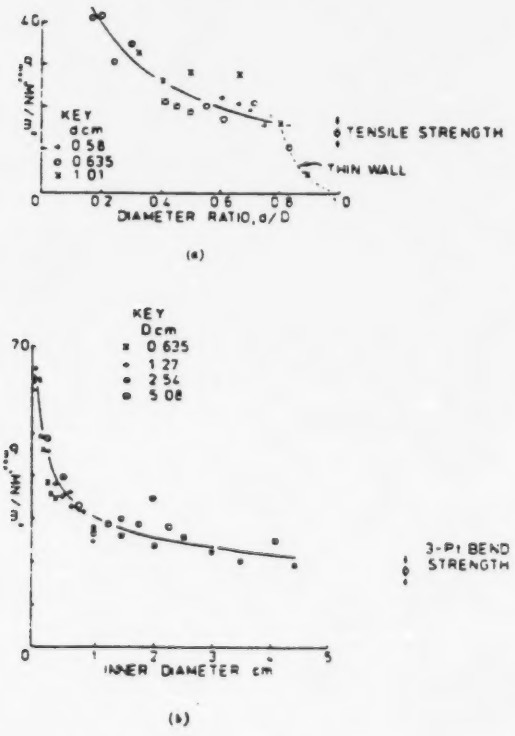

Figure 4.15 a) Internal pressure tests and b) Diametral tests, on ring specimens of graphite PI-6

This extensive work on graphite helps to refine the calculations based on the thick cylinder formula and to estimate the average mold life as a function of safety margin used. A nicer alternative would be to use a large piece of much stronger graphite. Ultra high strength graphite is available (at considerable cost) in smaller sizes but not in the large rounds that are needed in this application. Other techniques have been tried by others, such as forming the cylinders from a number of concentric matched shells, but none have been as successful in economic practice as using monolithic graphite, knowing its limits and staying just within those limits most of the time. Occasional breakage is accepted. Thus, the other side of the question is an accurate estimation (or measurement) of the stresses applied to the mold.

The amount of radial stress generated from uniaxial stress applied is not a priori known. For example, during cold pressing, anywhere from 25% to 80% of the axial stress may be transmitted to the radial direction depending on powder density and properties (see Figure 4.16). During hot pressing, this quantity may vary and will depend on the material properties such as Poisson's ratio, etc.

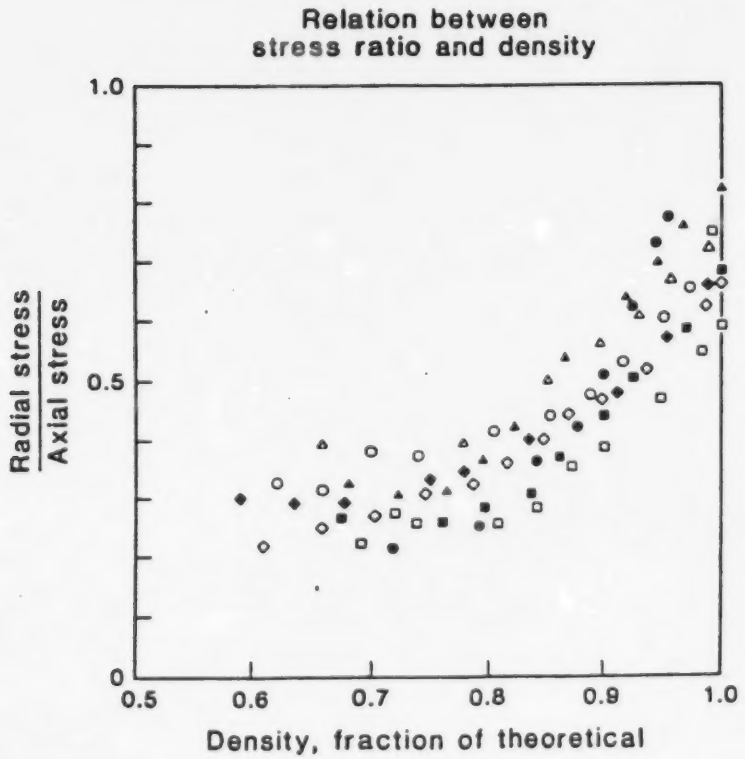

Figure 4.16 Relation between stress ratio and density

From [illegible] Relation of Axial and Radial Stresses to Powder Properties

If the sintering process involves particle volume increase through chemical reaction of additives or crystal phase changes, the forces on the die wall can exceed the ram applied pressure by a considerable factor. Even when such events are not occurring, there is some variation in the die wall transfer ratio with pressure, density, temperature, etc. In practice it is necessary to measure these forces under process conditions and then to design molds to withstand them.

The most effective method of measuring die wall forces under pressing conditions is to construct molds from a moderate-strength graphite and stress them to failure under process conditions. When reasonable statistics have been obtained, the data can be used to calculate stress limits appropriate for higher strength graphite molds. As discussed above, smaller-scale modelling of the situation is difficult to scale up to larger sizes as the strength of materials is peculiarly size dependant. The unfortunate aspect of this approach is that for each powder or blend of powders the expensive full-scale stress measurement must be undertaken.

Considerable success has been achieved at Electrofuel in controlling process parameters to avoid mold breakage by using previous breakage data to estimate the stresses actually present. Ram pressure is programmed through an empirical cycle as the pressing proceeds. Stress transfer is found, in general, to be maximum in an intermediate range of temperature. For several well known powders and part geometries the applied stress can safely set to within 10-15% of the estimated Weibull 50% breakage level with only a moderate rate of mold loss.

4.4.2 KINETICS OF HOT PRESSING

It is important to study the kinetics of hot pressing or densification rate for each material as that determines the productivity, and hence the economic viability of hot pressing that material. It is also important to determine the effect of process variables and composition (additives) on the densification kinetics. For these reasons, hot pressing kinetics of BN and composites were studied.

It is generally accepted that, at the start of a hot pressing operation, initial densification takes place via a particle rearrangement/fragmentation and grain-boundary sliding process. This is an important mechanism particularly during early stages of compaction and sintering, as well as at very high pressures and/or lower temperatures.

Murray et al.* proposed that densification during hot pressing proceeded by a plastic or viscous flow mechanism for which they derived the equation

$$\frac{d\rho}{dt} = \frac{3\sigma}{4} (1 - \rho)$$

where σ is the applied stress

η is the viscosity

and ρ is the fractional density.

* Murray et.al.(1954)

More recently, researchers have shown that hot pressing of most oxides (alumina, magnesia, etc.) was essentially diffusion controlled, occuring by bulk diffusion enhanced by the stresses due to hot pressing, or by Nabarro-Herring diffusional creep.

Rossi and Fulrath* based their rate equation on the Nabarro-Herring creep model in which the strain rate is expressed by

$$\sigma' = \frac{40\ D\ \Omega\ \varepsilon}{k\ T\ d^2}$$

where σ' = Strain rate (sec-1)
D = Diffusion coefficient (cm2 sec-1)
Ω = Volume of a vacancy (cm3)
ε = Effective stress (dyne cm-2)
k = Boltzmann's constant
T = Absolute temperature
d = Mean grain diameter (cm).

In order to apply this model to densification during hot pressing, a stress concentration factor was introduced to allow for the effects of the presence of pores (at low values of total porosity) on the effective stress and the constraint in creep rate exerted by the die wall, resulting in

$$\sigma' = \frac{40\ D\ P}{k\ T} \cdot \frac{b\ Q}{d^2}$$

where b = Stress concentration factor
P = Applied stress
Q = Porosity.

Consequently it was shown that for low porosities

* Rossi,R.C. and Fulrath,R.M.,J.Am.Cer.Soc.,48(11),558,1965.

$$\frac{dP}{dt} = \frac{40\ D}{k\ T} \frac{b\ P\ (1 - P)}{d2}$$

Thus, both plastic flow and enhanced diffusion lead to the same form of equation, i.e.

$$-\frac{dQ}{dt} = m\ Q$$

which on integration gives

$$\log Q = -m\ t + \log Q_0$$

Therefore, the final stage of hot pressing should show a linear relation in a log porosity versus time plot if temperature and pressure remain constant.

For boron nitride, pressing kinetics must be some mixture of the two mechanisms. The existance of the liquid B2O3 phase at a level of about 4% can well be expected to give a viscous flow behaviour and this can be clearly seen as the temperature is increased through the 1000 degrees C range where the viscosity of B2O3 is rapidly decreasing. Near the end of the pressing cycle when considerable solid BN/BN bonding has taken place and densification rates are significantly slower. pressure enhanced diffusion may well be important.

Using the ram travel as a function of time it is possible to measure the densification kinetics, and these are routinely analyzed to give time constants (m in the equation above). An example is given in the following figures. showing successive stages in the analysis.

RAM TRAVEL VS. TIME

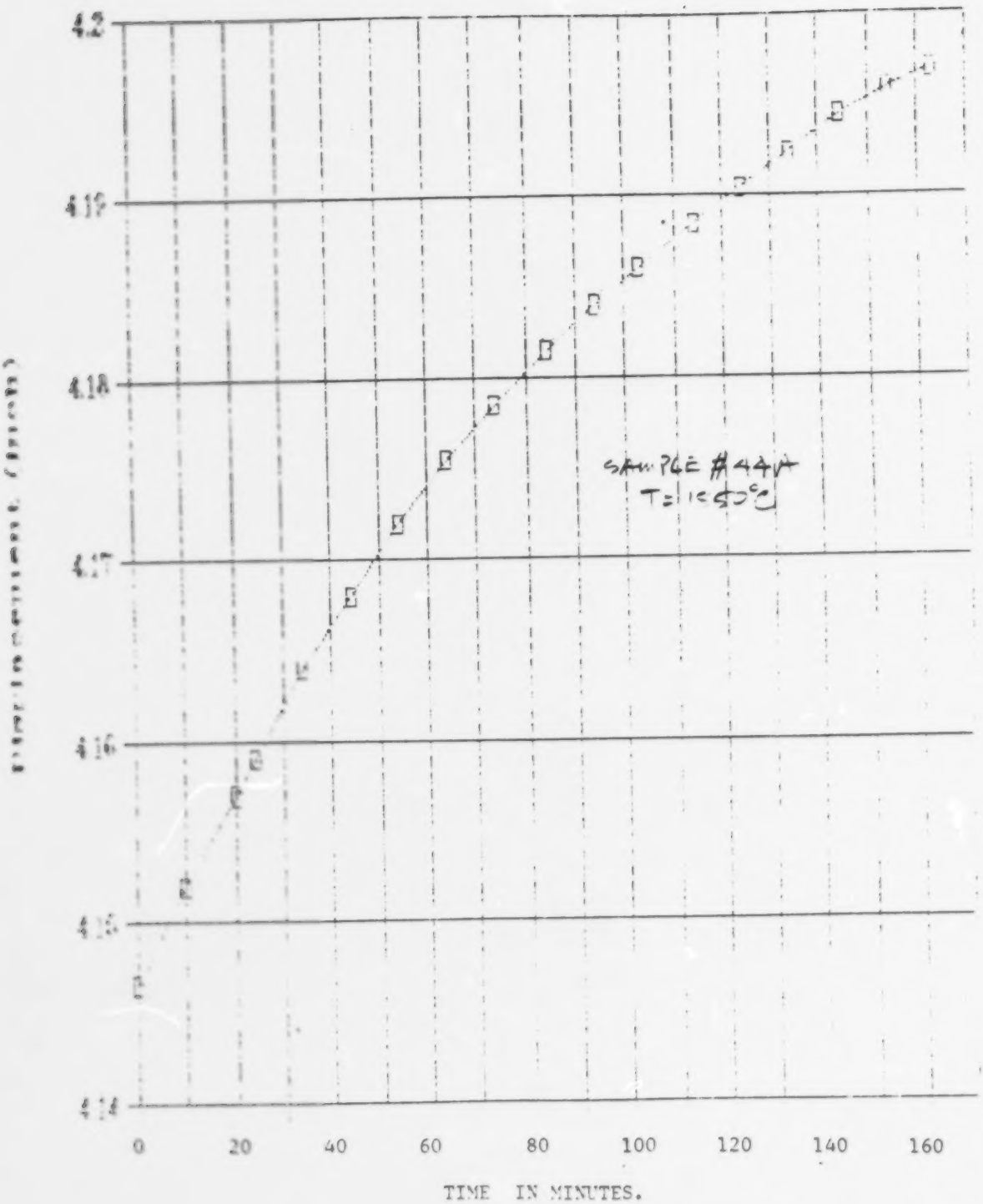

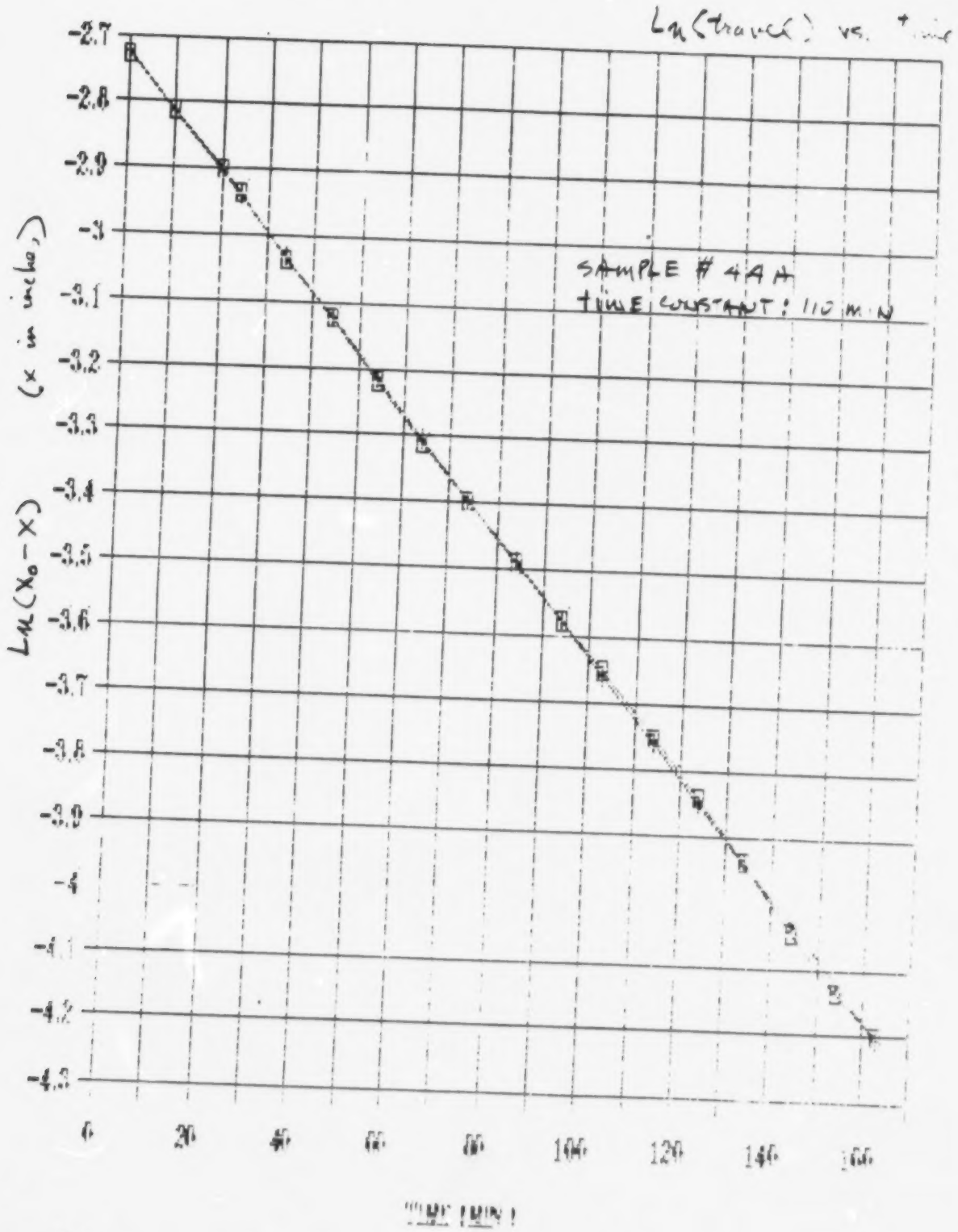
Ln(track) vs. time
SAMPLE # 4A H
TIME CONSTANT: 110 MIN
Ln(X₀ - X)
(x in inches)
-2.7
-2.8
-2.9
-3
-3.1
-3.2
-3.3
-3.4
-3.5
-3.6
-3.7
-3.8
-3.9
-4
-4.1
-4.2
-4.3
0
20
40
60
80
100
120
140
160
TIME (MIN)

5. FINISHED PART CHARACTERISTICS

5.1 MONOLITHIC BORON NITRIDE

5.1.1 STRUCTURAL ANALYSIS

Using Cuk_{α} radiation the X-ray diffraction patterns of BN hot pressed solids were recorded. All patterns show the maximums coresponding to the hexagonal structure. The peaks with (101), (102), (110) and (112) Miller's indices are split into doublets. The slittings and the extra peak corresponding to an interplanar distance of 3.15 Å are similar to those of active BN powder and could be explained by turbostratic defects of the structure and sp2 hybridization. The X-ray diffraction pattern of a hot-pressed BN compact is shown in Fig.5.1.

The values of lattice parameters were determined from (110) and (112) lines and were found to be a= 2.507 Å and c= 6.668 Å.

In comparison with the initial powder's lattice parameters, the value of 'a' is practically the same and the 'c' value is increased by hot-pressing. The graphitization index R calculated from the (100), (101) and (102) lines was found to be 1.66, a lower value than that of active BN powder, but higher than that obtained for non-active powder. The graphitization index of analysed hot-pressed BN compacts was found to be in the range 1.60 to 1.90 for well densified samples, which shows a well ordered structure in these cases. For cracked BN compacts, the graphitization index was found higher than for active powder (R=2.75), showing a high level of structural defects which determine the microcracks.

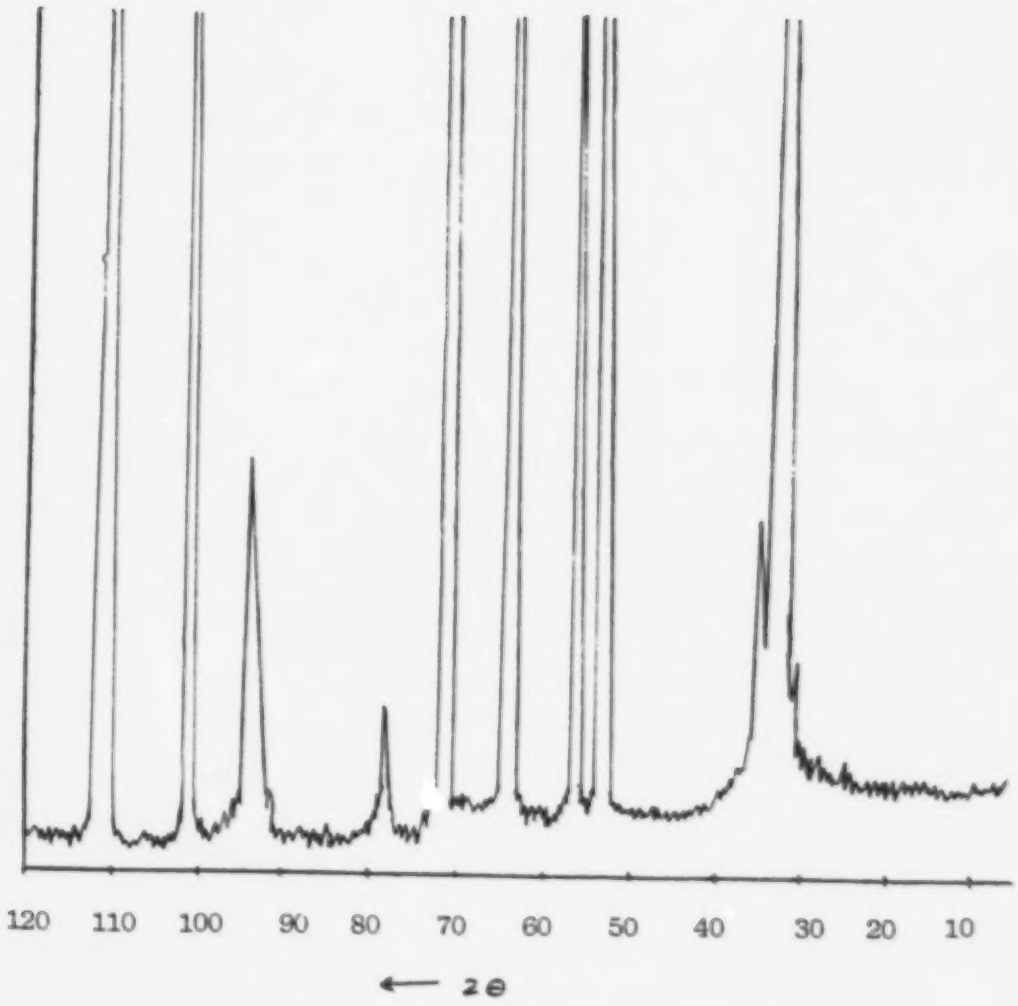

Fig.5.1 X-ray diffraction pattern of hot-pressed BN compact, having a hexagonal structure.

In order to determine the anisotropy of crystallite orientation in hot-pressed BN ceramics. Samples were cut from a single block so as to expose surfaces parallel to the pressing direction and perpendicular to the pressing direction. Using the monochromatic Fek_{α_1} radiation, the X-ray diffraction patterns for both samples were recorded in the same experimental conditions (same incident intensities, range, time constant, goniometer speed and paper speed). In fig.5.2, the x-ray diffraction patterns of both samples are shown.

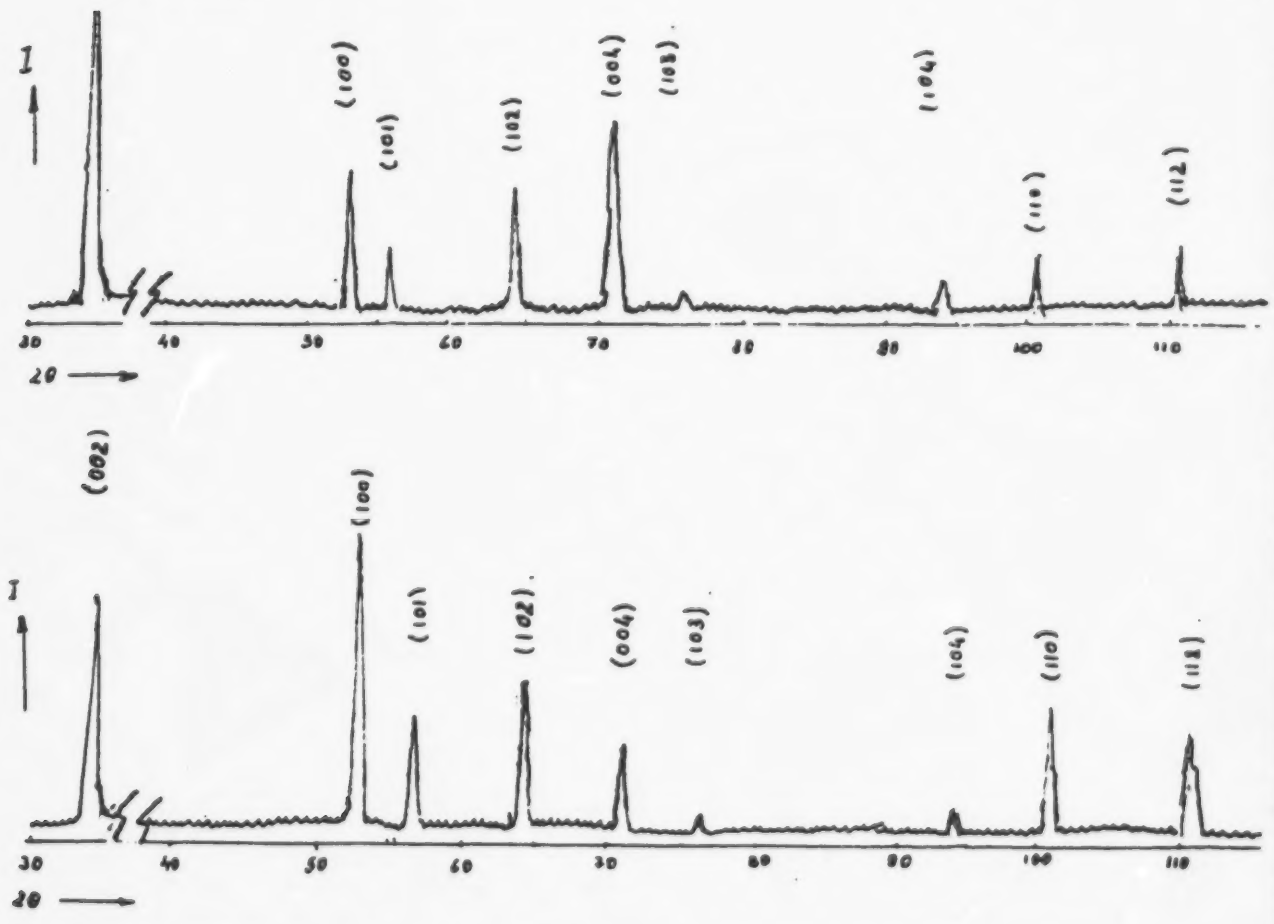

Fig.5.2 X-ray diffraction patterns in the perpendicular and parallel directions (with respect to the pressure applied in hot-pressing) showing different intensities of the maximums

Both samples have hexagonal structure and the lattice parameters are equal. The difference between intensities of the maximums appeared due to the orientation of the hexagonal structure during the hot-pressing process. The ratio between the perpendicular and the parallel direction intensities coresponds to the value of crystallite orientation.

$$I_{perp} / I_{par} = 2.76$$

Thus the hexagonal unit cell orient preferentially under the pressure.

This leads to the situation depicted in fig. 5.3.

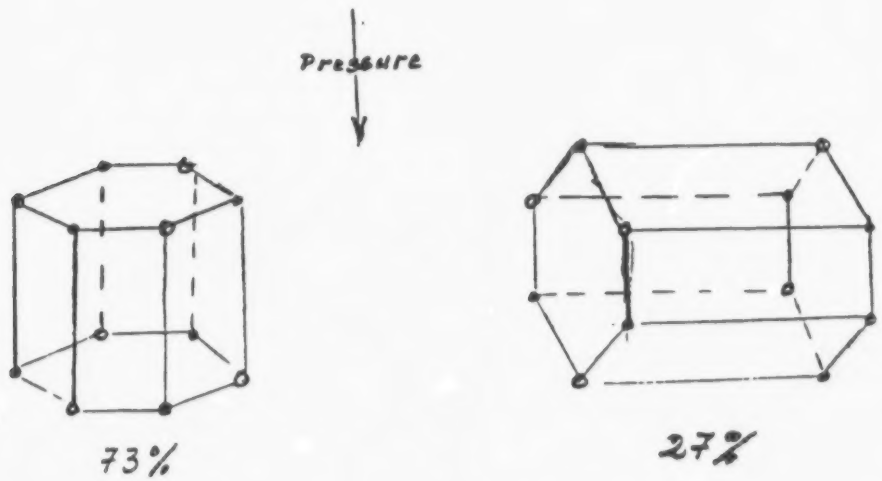

Fig 5.3 Crystalline orientation of hexagonal structure in hot-pressed BN ceramics

The graphitization index is higher in the parallel direction than in perpendicular direction. which show also the difference between the number of structural defects in these two directions.

The ratios between (200) the peak intensities in the perpendicular direction and parallel direction were recorded and this ratio was plotted versus depth for different positions along the radius of the hot-pressed disk. The ratio between X-ray intensities. proportional to the crystallite orientation, gives us an idea of the spatial variation of crystallite orientation over the whole hot pressed compact.

Fig.5.4 Variation of X-ray intensities ratio versus position in hot-pressed BN ceramic

Fig 5.4

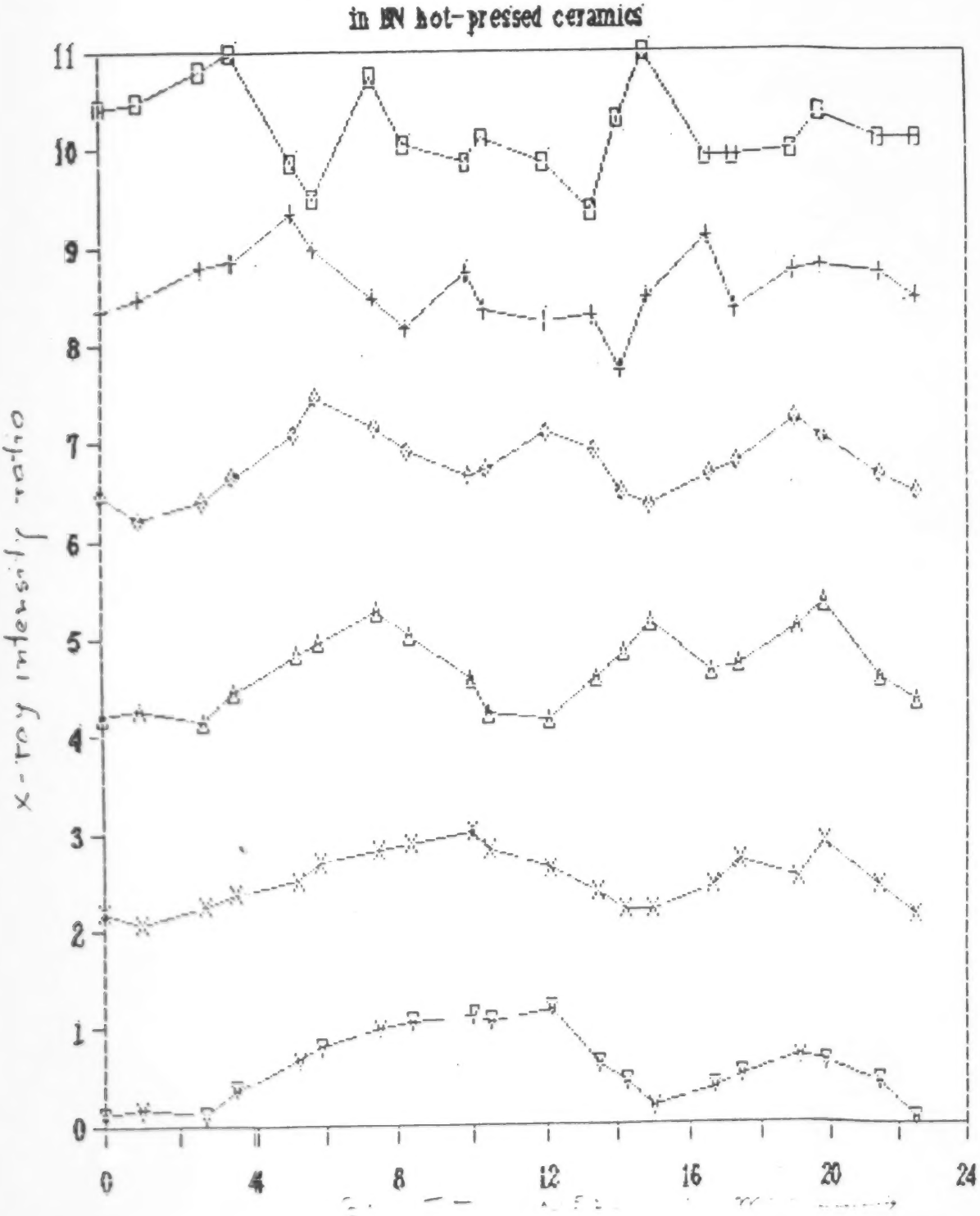

A careful look at Figures 5.4 will give an indication of the orientation contours in the part. These contours show the same conical cap configuration predicted in the cold-pressing analysis with some evidence of densification bands. The part is highly oriented near the center and has reverse orientation in edge regions and in several spots along the cylindrical edge. Because of the inherent anisotropy, orientation is easily measured in boron nitride. It is an ideal medium for establishing the detailed flow and densification behaviour of ceramics during hot pressing.

5.1.2. MICROSCOPY.

Using scanning electron microscopy, some structural features of BN hot-pressed compacts were obtained.

The secondary electron image of BN hot-pressed compacts show the re-arrangement of the crystallites under pressure, which is correlated with the crystallite orientation. This effect can be seen in the SEM micrographs shown below. The pressure direction is indicated by the arrow.

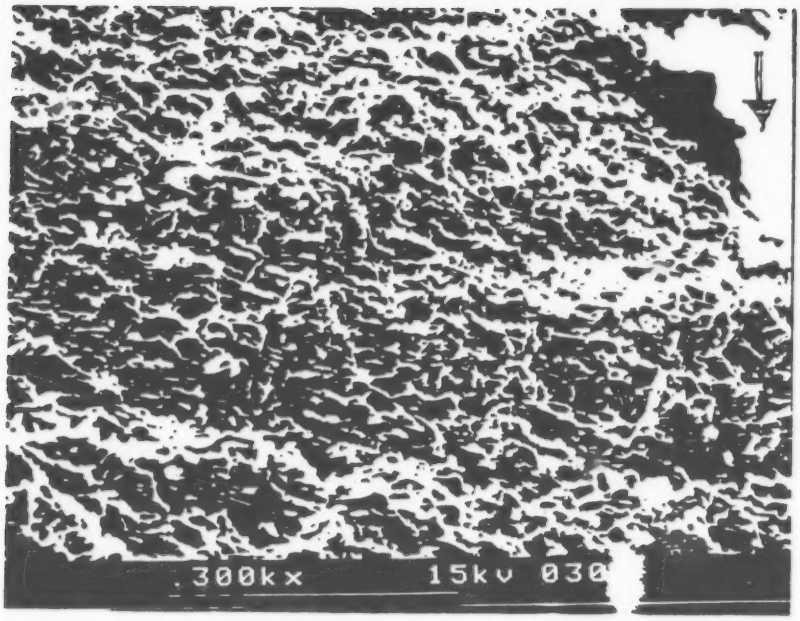

Fig. 5.5 Scanning electron micrograph of BN hot-pressed compact

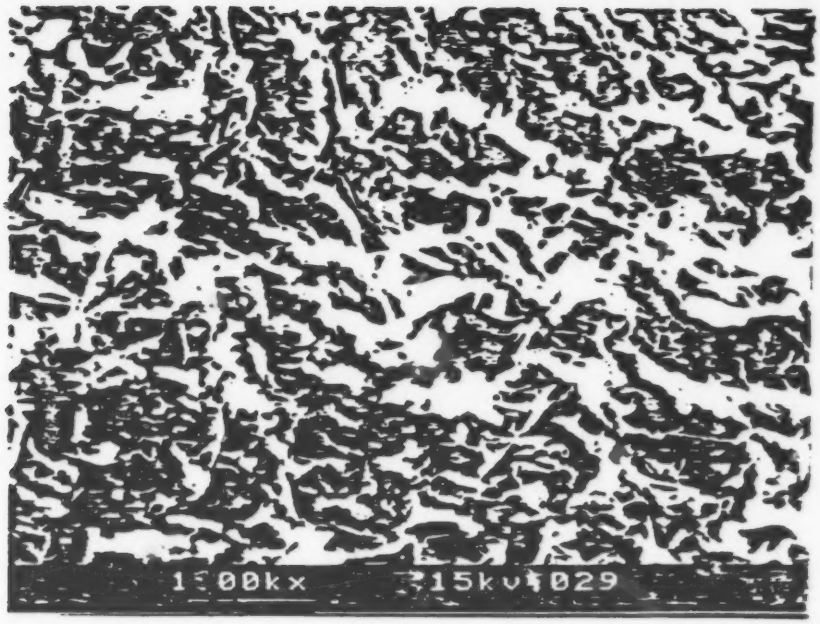

Fig. 5.6 Scanning electron micrograph on the fractured BN compact parallel with the pressure

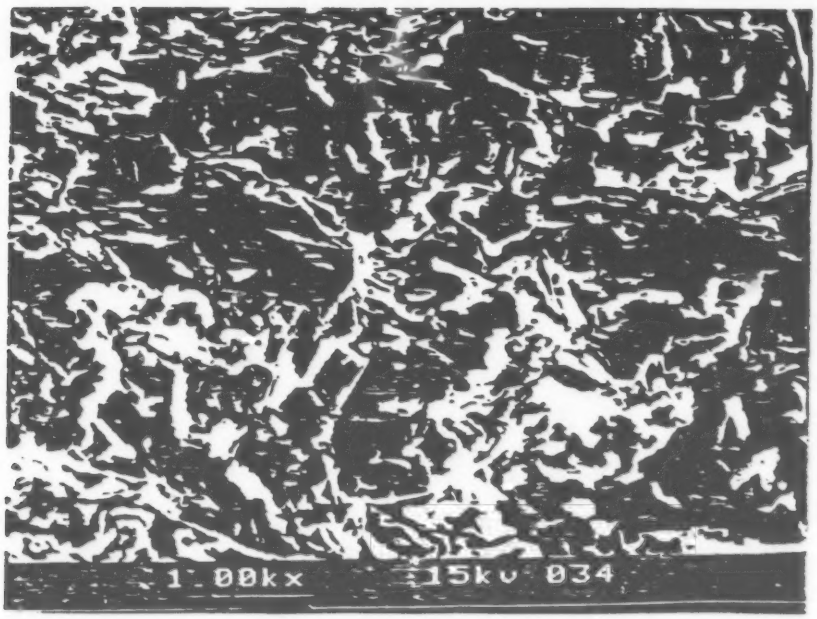

Fig. 5.7 Secondary electron images of BN hot pressed ceramics

Fig. 5.8 Microfracture of BF compacts with preferential orientation of the flakes under the pressure.

5.1.3 STRENGTH

The strength of samples was measured in a 3-point bend apparatus both at room temperature and at elevated temperatures. The values obtained are strongly dependant on position in the sample disk and orientation, as expected from microstructural and X-ray analysis. The range for well densified samples lies between 12.000 psi and 20.000 psi. In addition to the dependance on orientation, there is a further dependance on grain size. Samples pressed from powders with large, strong and well oriented agglomerates show lower strength than those pressed from loosely agglomerated powders. A comparison of strength of fine-grain well densified material with that of other manufacturers is shown in the following figure.

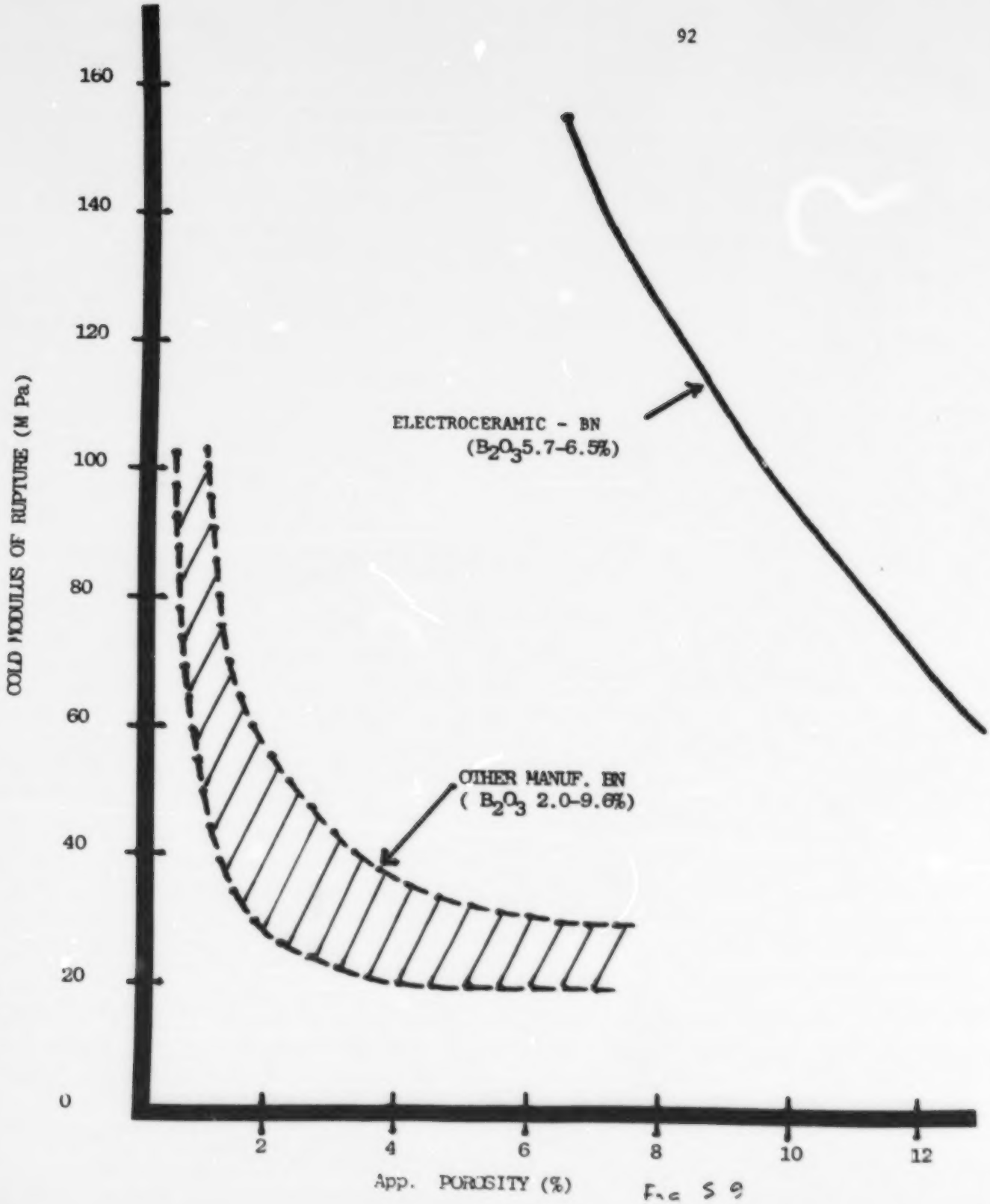
160
140
120
100
80
60
40
20
0
COLD MODULUS OF RUPTURE (M Pa.)
ELECTROCERAMIC - BN
(B_2O_3 5.7-6.5%)
OTHER MANUF. BN
(B_2O_3 2.0-9.6%)
2
4
6
8
10
12
App. POROSITY (%)

Fig 5 9

5.2 BN/BN COMPOSITE

BN solid/ fibers ceramic composites were prepared by blending prepared powder with chopped BN fibre, cold pressing and finally hot pressing.

Cold pressed samples were analysed by scanning electron microscopy to obtain data concerning the mixture. Samples with either random orientation or high orientation of BN fibers could be obtained, using two different mixing procedures. In Fig 5.10 micrograph of a random orientation BN fiber compact is shown and in Fig. 5.11 a micrograph of an oriented fiber compact is given, both samples having been cold pressed under the same conditions.

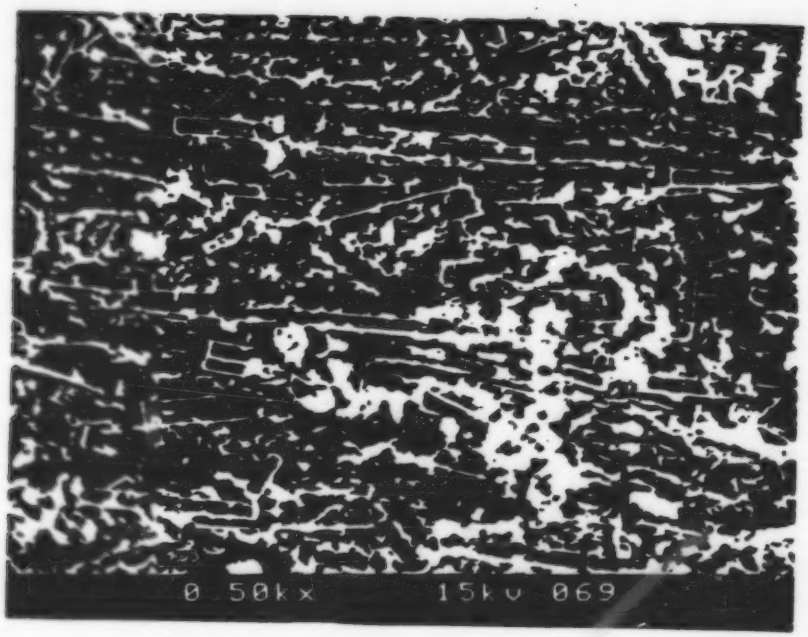

Fig. 5.10 Secondary electron image of BN/BN composite with random orientation of fibers

Fig 5.11 Secondary electron image of BN/BN composite with oriented fibers

The micrographs show an uniform distribution of BN powder among the fibers.

The BN/BN composite hot-pressed samples were analysed by X-ray diffraction and SEM. X-ray diffraction analysis shows highly oriented BN samples, the amorphous character of the fibers having disappeared. The X-ray diffraction pattern obtained with monochromatic Fe k_{α_1} radiation is shown in Fig. 5.12.

The maximums correspond to a hexagonal structure with high intensities for the (001) type reflections.

The scanning electron microscopy images of fracture surfaces in the perpendicular and parallel directions with respect to fibers orientation are shown in Fig. 5.13; 5.14; 5.15.

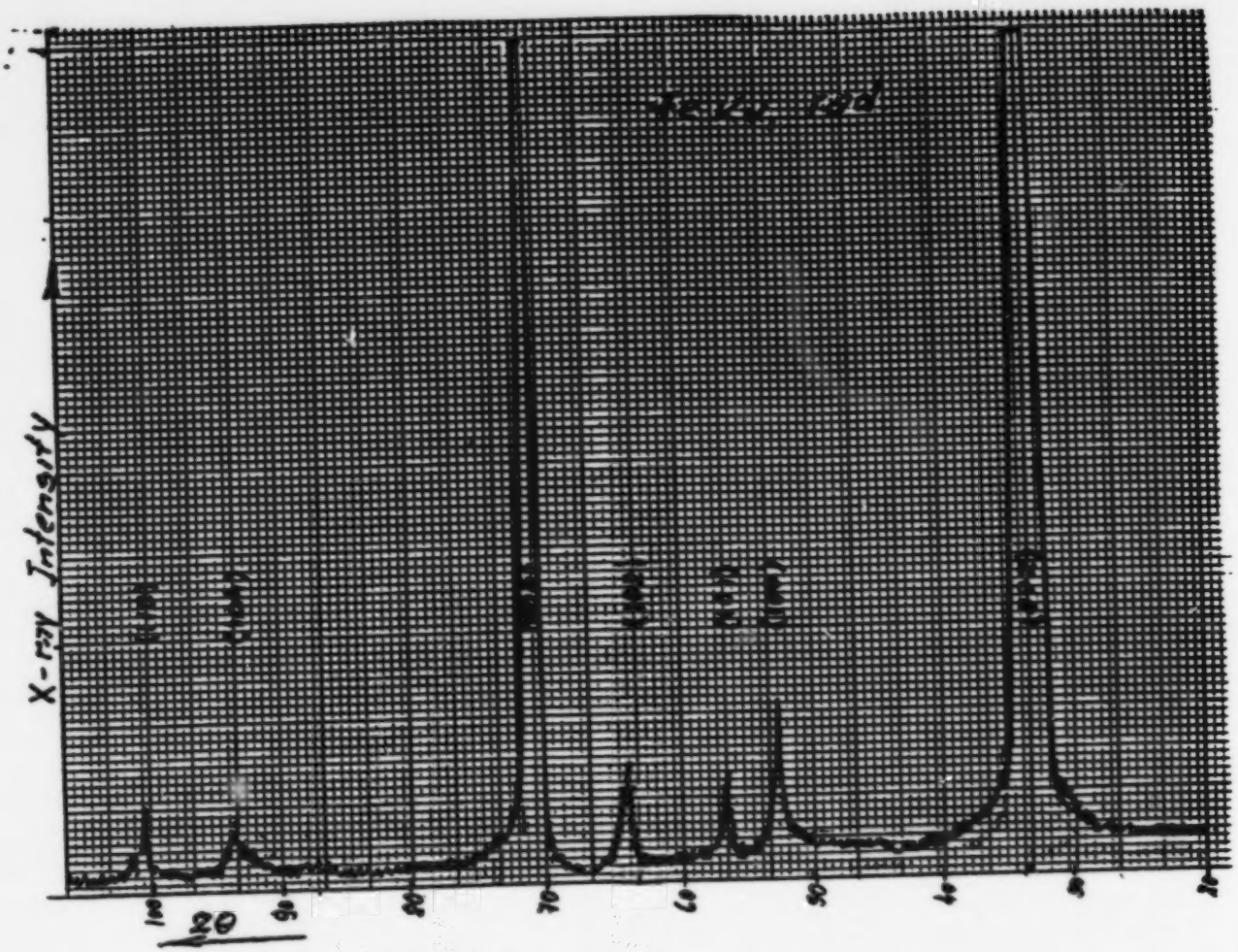

Fig 5.12 X-ray diffraction patern of BN/BN composite ceramic

Fig 5.13. Secondary electron image of fractured UD/UD composite parallel with a fibers orientation

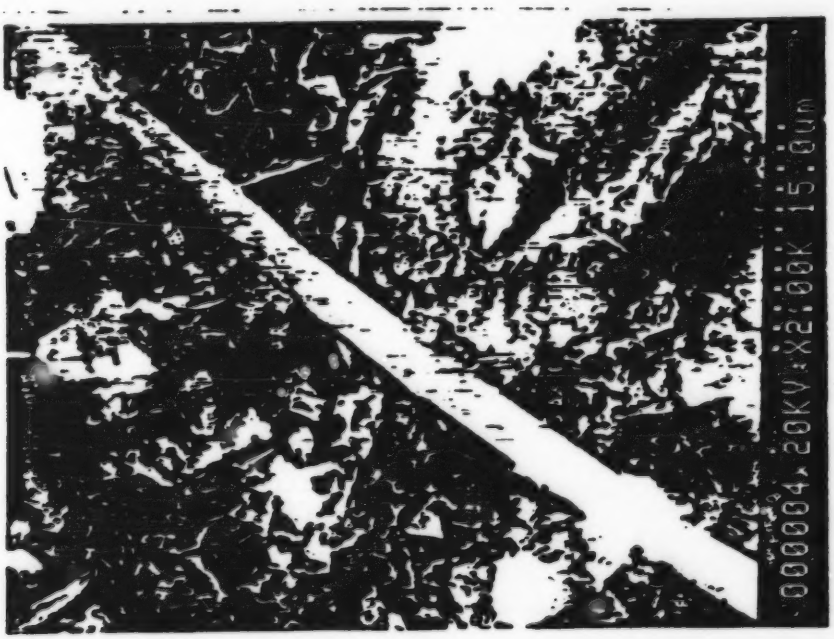

Fig 5.14 Scanning electron microfracture along a fibers.

Fig 5. 15 Secondary electron images of BN/BN fracture in perpendicular direction with fibers orientation.

The fracture surfaces parallel to the fibre orientation show well densified material and the typical oriented BN flakes. In the fracture phase perpendicular to the fibre orientation the broken ends of the fibres can be distinguished from the matrix only by their apparently larger grain size. No pull-out is evident as might be expected from the excellent bonding afforded by the residual B2O3 and BN/BN bonding itself. The fibres have become highly crystalline and ordered as a result of the hot pressing procedure.

Strength measurements on the BN/BN composite samples show extreme anisotropy as might be expected. Three-point bend **modulus** of rupture was less dependant on pressing direction than on fibre orientation, showing that the fibre structure continued to play a significant role even after hot pressing (which caused great amounts of fibre fracture). While showing improvement over monolithic BN, the strengths of the BN/BN composites showed less improvement than had originally been anticipated. Table 5. shows composite material average strengths in two orthogonal directions.

Table 5.

Orientation with respect to fiber	3-point MOR (psi)
Perpendicular	19,500
	9,000

Although the tensile strength of the BN fibre starts out much higher than that of BN solid its properties may be degraded in the processing procedures. Strengthening and toughening due to crack deflection and fibre pull-out are less effective in BN/BN fibre composites than in other composites with BN fibre (such as Al2O3) because of the tight BN/BN bonding and good match of thermal expansion coefficient.

5.3 PARTICULATE COMPOSITES

Several particulate composites were prepared to meet the requirements of an aluminum evaporator boat. These composite electroconductive ceramics can be heated directly by passing an electrical current through them, much as would be possible with metals or graphite (which are, however, attacked by molten aluminum). The resistivity can be tailored by controlling the percentage and distribution of the electroconductive phase.

From a microscopic point of view, the electroconductive and insulating phases of ceramic conductor-insulator composites have a non-uniform distribution, and the particle size and mixing procedure of the starting powders have a marked effect upon the properties, especially resistivity. In some cases local microcompositional fluctuations lead to high local heating in use. The temperature rises abnormally under such conditions and severe erosion occurs in the affected area, thereby shortening the life of the evaporation source. Taking into account this aspect, a careful technological process producing an uniform distribution of the electroconductive phase will achieve composites with extremely stable and uniform properties.

Two different type of BN electroconductive ceramics were evaluated for boats used in aluminum metallizing.

* BN-TiB2 binary composite
* BN-TiB2-AlN ternary composite

The starting BN powder used in these composites preparation contains 4.3% wt B2O3 with the B2O3 binder playing an important role in the sintering process. The TiB2 being electroconductive, determines the electrical conductivity of the composite. Powders supplied by different manufacturers yield different conductivities. The particle size and range play very important roles in this regard.

The mixed, dried powders were cold pressed into graphite molds (2.5" diameter) for hot pressing. Various pressures and sintering temperatures were chosen and for each sample the sintering data were analysed.

Sintering kinetics of these materials were studied by recording the ram position versus time at various pressures. Examples for BN binary and ternary electroconductive composites are shown below. (Fig. 5.6a) and 5.7a,b).

Figure 5.14a. Sintering graph of a binary electroconductive ceramic

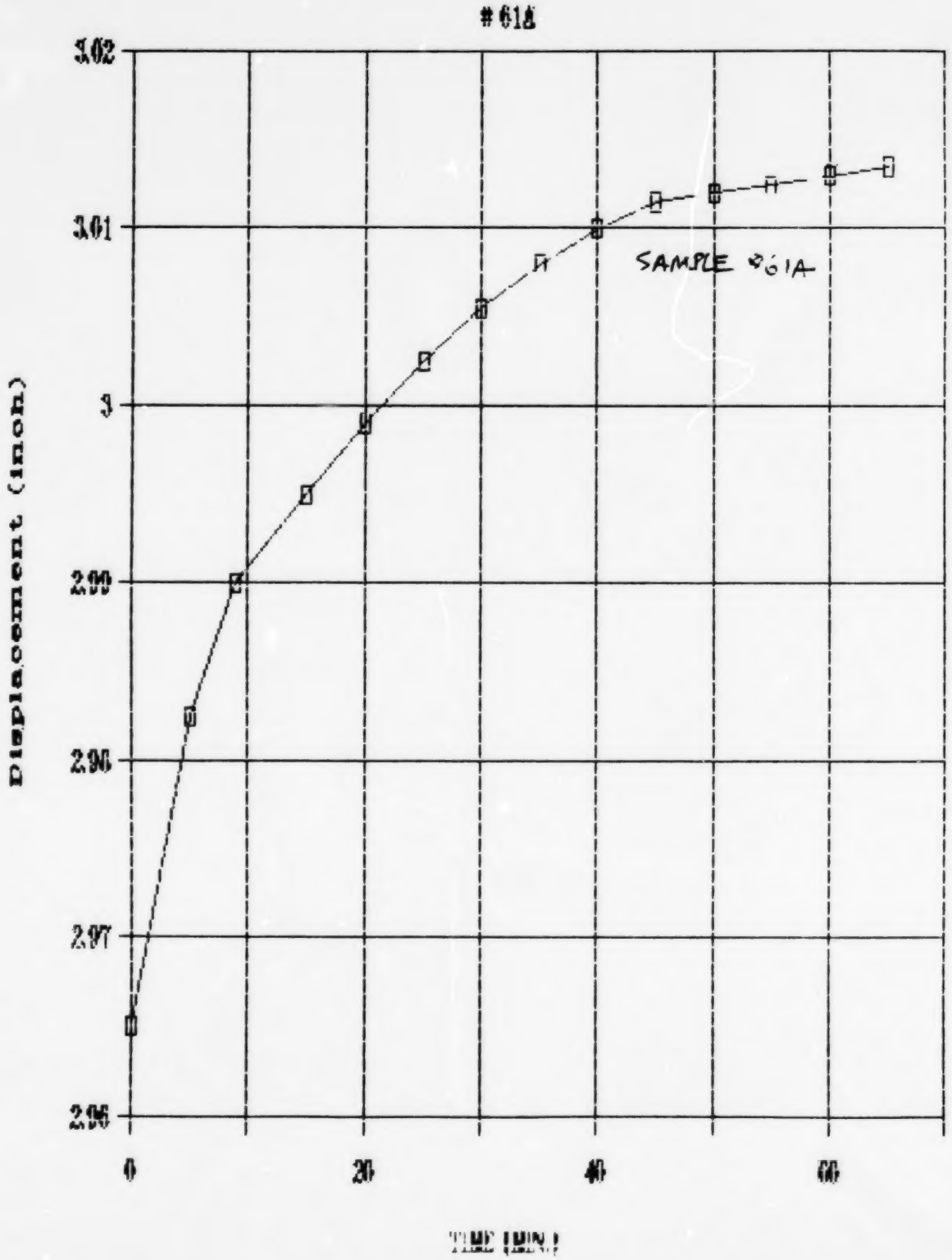

Figure 5.46b. Logarithmic variation of ran position for the same sample

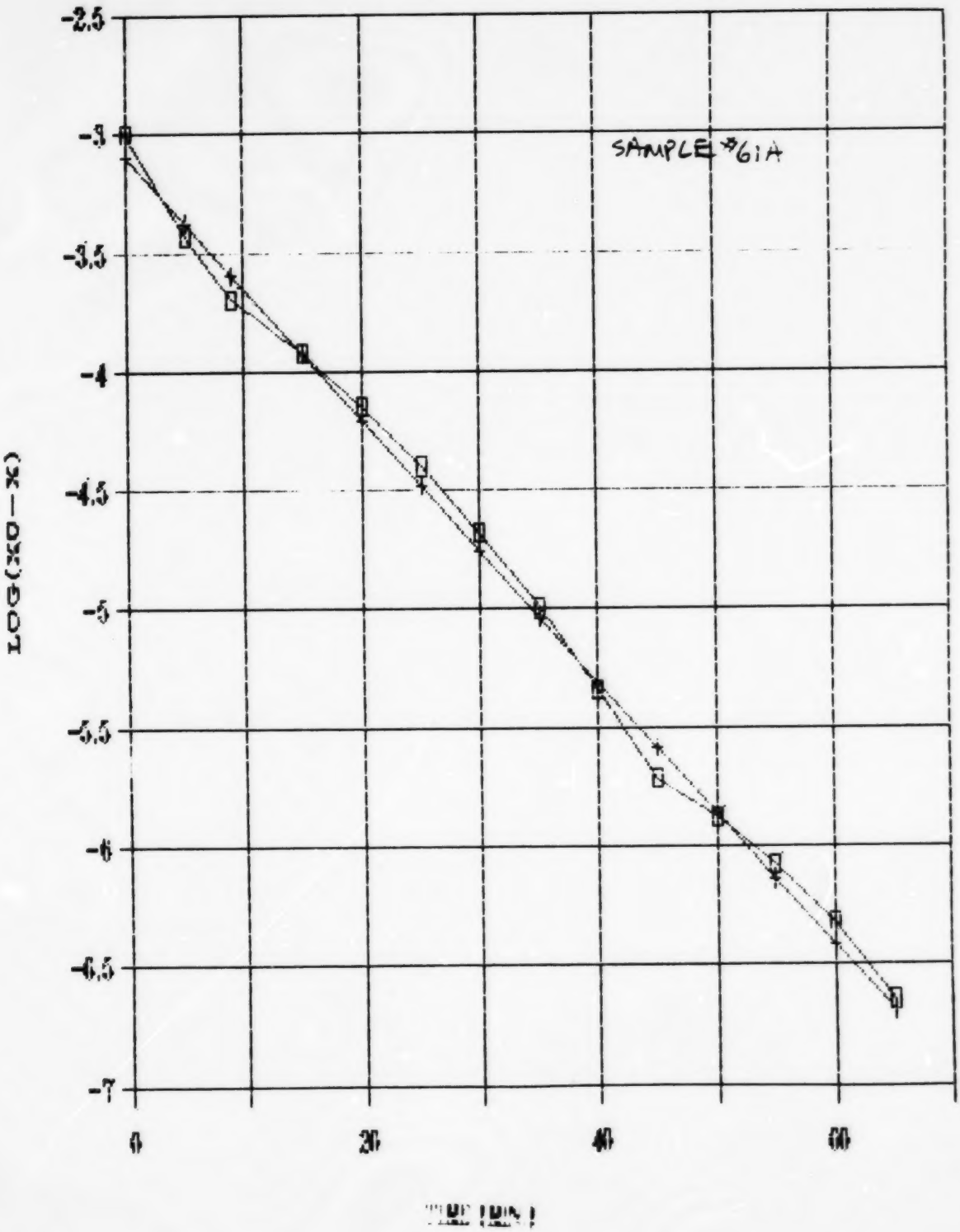

Figure 5.17a. Sintering-curve of a ternary BN composite

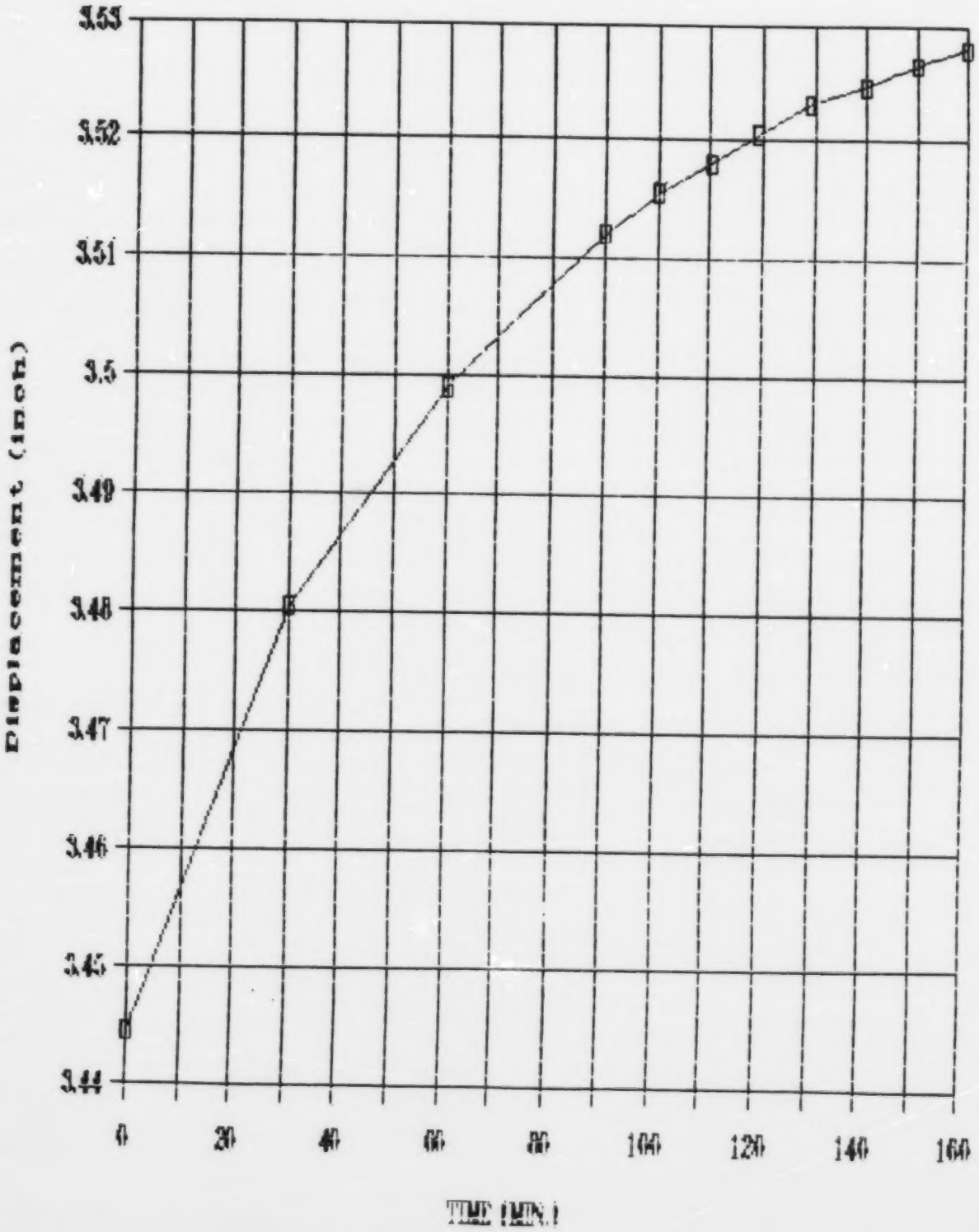

Figure 5.17b. Logarithmic variation for time constant determination

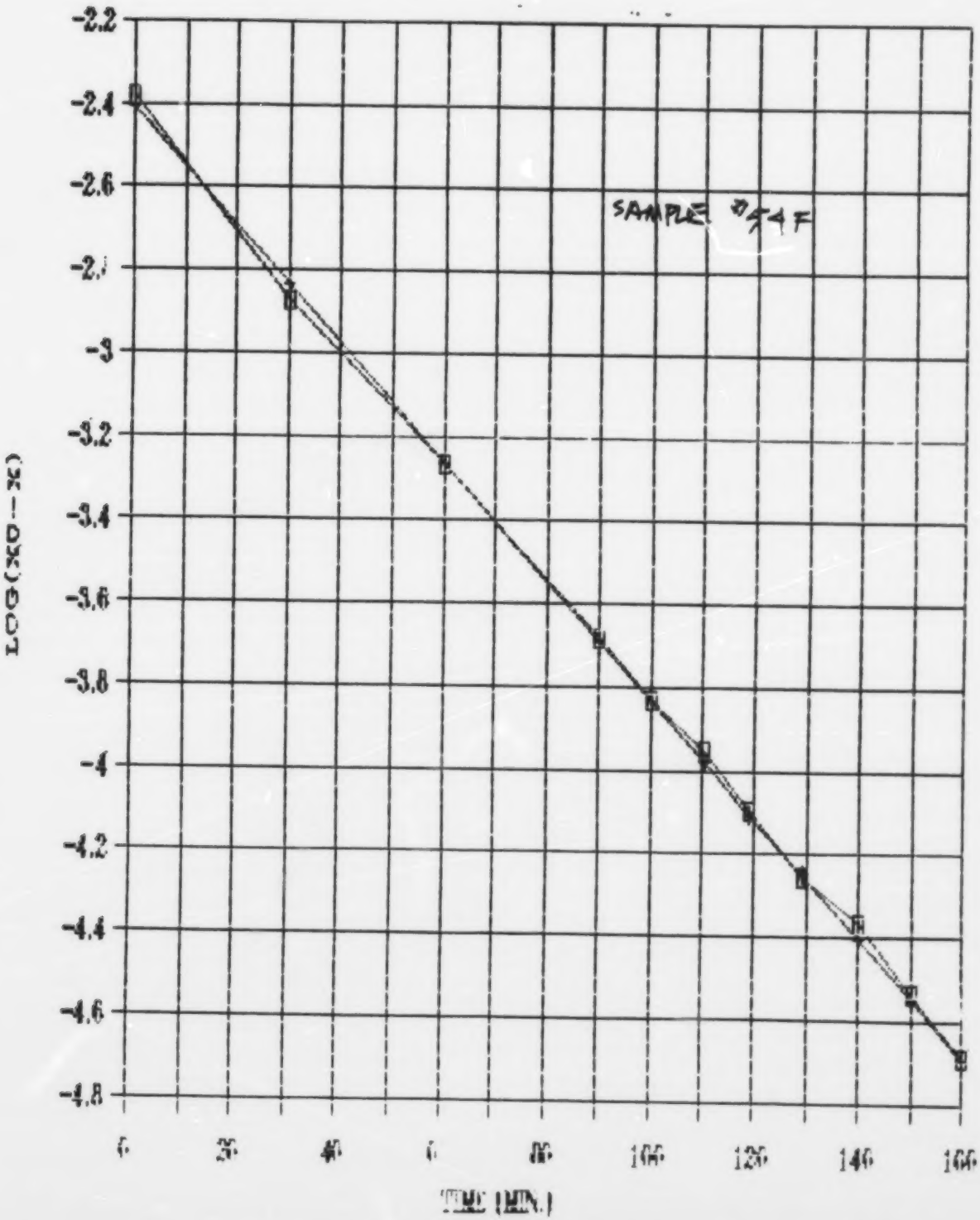

Using Cuk$_{\alpha}$ radiation, the X-ray diffraction patterns of BN electroconductive hot pressed ceramics were recorded. In the case of ternary BN/TiB2/AlN electroconductive composite, the X-ray diffraction shows the maximums corresponding to all three starting compounds, having slightly modified positions compared with those of the starting materials. In Table 5.1, the interplanar distances from the diffraction patterns of the electroconductive BN composite and of the BN, TiB2, AlN starting powders are listed.

Composite ceramics	BN powder hexagonl structure		TiB2 powder hexagonal structure		AlN powder hexagonal structure	
	a=	c=	a=	c=	a=	c=
dhkl	dhkl		dhkl		dhkl	
3.3485	3.33	(002)				
3.2433			3.22	(001)		
2.7183					2.693	(100)
2.6329			2.62	(100)		
2.5020					2.490	(002)
2.3829					2.373	(101)
2,1784	2.17	(100)				
2.0580	2.06	(101)				
2.0354			2.033	(101)		
1.8320	1.817	(102)			1.828	(102)
1.6737	1.667	(004)				
1.6173			1.613	(002)		
1.5634	1.555	(110)			1.555	(110)
1.5161			1.514	(110)	1.494	(111)
1.4166					1.414	(103)
1.374 (102)						
1.3747			1.370	(111)		
1.3447					1.3467	(200)
1.3278	1.325					
1.3094			1.311	(200)	1.3125	(112)
1.3035	1.301				1.3006	(201)

Table 5.1 Interplanar distances of x-ray diffraction pattern of ternary electroconductive composite ceramic and starting ceramic powders

The X-ray diffraction pattern of one binary composite (BN. TiB2) is shown below (Fig.5.18 and the presence of the major phases (BN.TiB2) can be seen by the maximums corresponding to their interplanar distances. The major phases have the hexagonal structure, slightly modified from the structure given in the ASTM files.

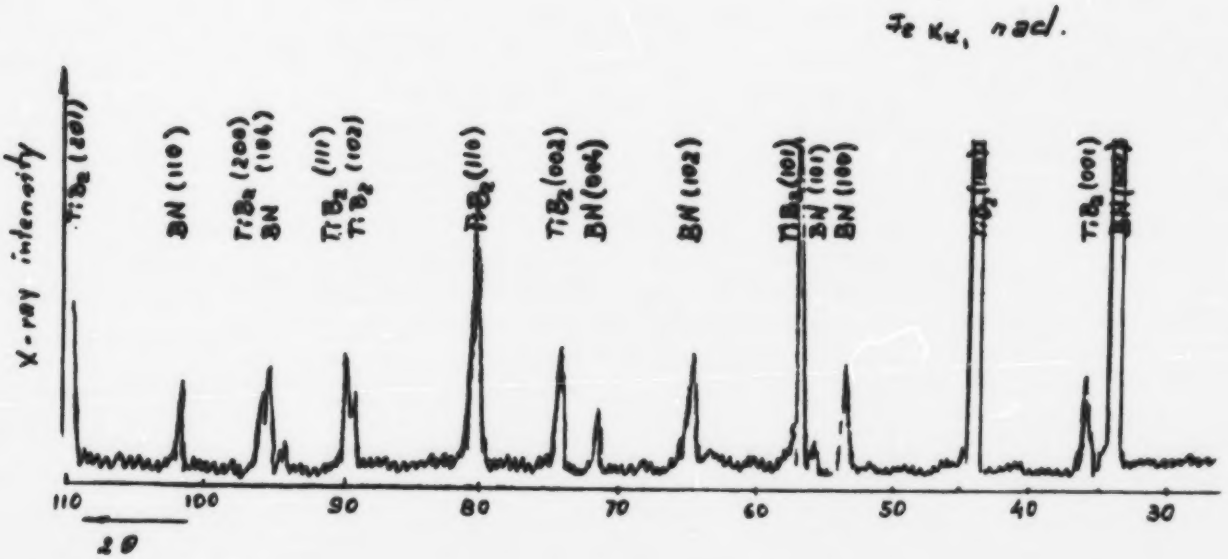

Fig 5.18 X-ray diffraction pattern of BN composite ceramic (45/55 of BN/TiB_2 compositional ratio).

Optical and Scanning Microscopy of polished and fractured surfaces were used to study the microstructure of the samples.

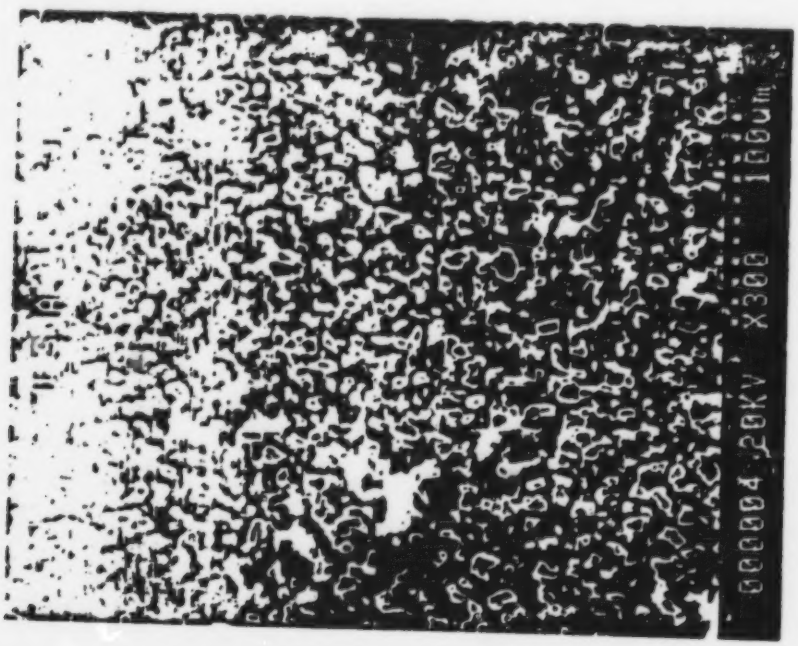

FIG. 5.19 Microstructure of ternary BN composite ceramic (x100)

FIG.5.20 Optical microstructure of binary BN electroconductive composite (x100)

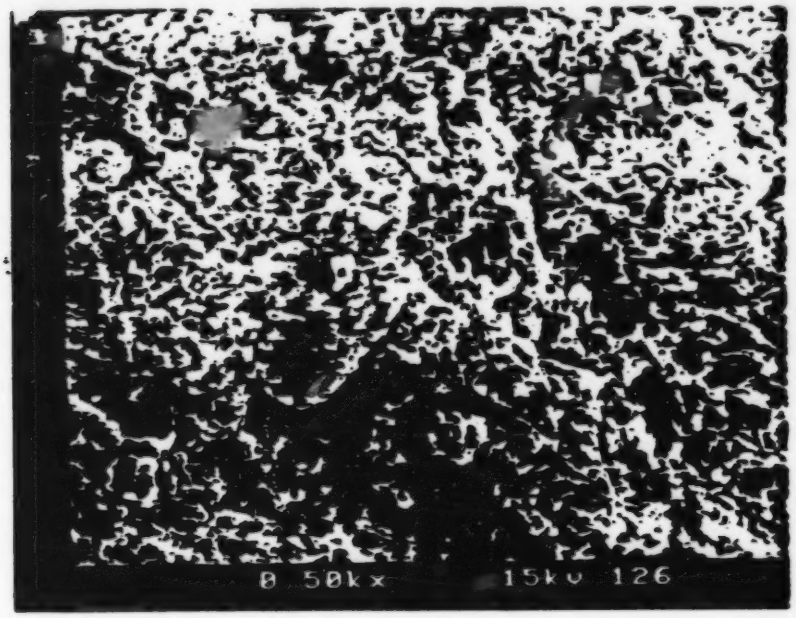

FIG. 5.21 Secondary electron image of binary BN composite

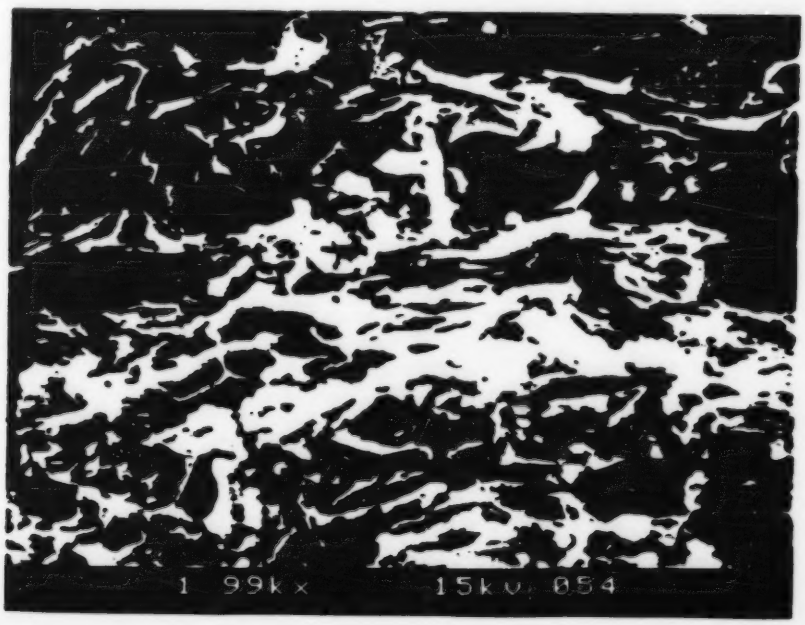

FIG. 5.22 Scanning electron micrograph of fractured BN electroconductive composite.

The microstructure of the ternary BN composite (Fig.5.19 shows well dispersed TiB2 particles, mainly in a BN matrix and with non-uniform AlN islands holding titanium diboride. AlN lumps cause micro compositional non-homogenity which affects the physical properties of the composite.

The optical images Fig.5.20 and SEM Figure 5.21 of the BN/TiB2 composite show a well dispersed electroconductive phase in the BN matrix.

The secondary electron image (Fig.5.22) clearly shows the BN flakes which hold the TiB2 particles. The sintering process seems to proceed in two stages: A BN sintering stage is followed by TiB_2 sintering with the TiB_2 particles getting rounded off in shape.

The macroscopical properties of the BN electroconductive ceramics are strongly connected with the microstructural aspects. Considering the microstructural aspects pointed out above, a characterization of physical properties of the binary composite was performed. The electrical resistivity was measured for 8 samples cut from a bulk specimen in order to detect possible variations due to the microcompositional variation.

The electrical resistivity of the composite ceramics was obtained in the range of 200 $\mu\Omega$.cm to 3000 $\mu\Omega$.cm as a function of the compositional ratio between the conductive and nonconductive ceramic component. Table 5.2 gives an example of the measured properties [density, electrical resistivity (room temperature), flexural strength (room temperature) and hot strength].

Sample #25 Heat no.164

Composition:	BN	TiB2	Others
wt.%	52	48	? at total wt.
vol.%	66.24	30.57	3.19

Density Theoretical:2.981g/cm3 Experimental:2.821g/cm3 Densification:94.65%

Sample:	Dimensions:	Resistivity:	Strength(20oC):	Strength(1000oC)
#25a	a=0.192'' c=0.228''	515 μΩcm	25,346 parallel	
#25b	a=0.185'' b=0.225''	528 μΩcm		5.544
#25c	a=0.205'' b=0.204''	509 μΩcm	23.124 perpendicular	
#25d	a=0.205'' b=0.229''	497 μΩcm		7,124
#25e	a=0.199'' b=0.223''	559 uΩcm		6.869
#25f	a=0.199'' b=0.227''	573 uΩcm	23,204 parallel	
#25g	a=0.169'' b=0.198''	596 uΩcm		6.432
#25h	a=0.209'' b=0.228''	586 uΩcm	20.588 perpendicular	

Table 5.2 Physical properties of binary BN composite ceramic #25

The density determinations by weight and volume measurements indicated good densification, the experimental values being in the range of 93% to 96% of the theoretical value, which gives a global porosity in the range of 4 to 7%.

The flexural strength measurements were performed in the parallel and perpendicular directions with respect to the applied pressure and the values found for parallel direction were smaller than for perpendicular direction. This fact could be explained by the previously shown structural orientation of BN due to hot pressing and to BN bonding in these ceramics.

The resistivity measurements show good compositional homogenity. For different lengths,the measurements give practically the same values in non-agglomerated and some agglomerated samples. The variation of current throughout the sample is proportional to voltage. In table 5.3 the current, voltage, and computed resistivity values are listed for a non-agglomerated TiB2 binary composite.

Table 5.3 Resistivity and strength values of BN electroconductive composite

Sample 5b

L(1)= 4.25

I(A)	U(mV)	r(IX)	
0.10	.0007	5.680747E-04	
0.20	.00135	5.477864E-04	Paralllel direction with pressure 13.565
0.30	.00201	5.437287E-04	
0.40	.00266	5.39671E-04	
0.50	.00332	5.388595E-04	
0.60	.00404	5.464338E-04	Perpendicular direction with pressure 15.80
0.70	.00462	5.356134E-04	
0.80	.00532	5.39671E-04	
0.90	.00597	5.383184E-04	
1.00	.00662	5.372364E-04	
1.10	.00728	5.370889E-04	
1.20	7.950001E-03	5.376422E-04	
med.	5.425104E-04		

The values obtained for resistivity were higher for agglomerated TiB2 samples, than for most non-agglomerated one.

One of the agglomerated TiB2 samples had substantially different values for resistivity along the pressure direction, which has been explained by compositional inhomogenities occurring in the mixing process. The studied samples have lower hardness making them easier to machine.

6 CONCLUSIONS

* Boron nitride based particulate composites have properties which can be tailored to meet specific application requirements. Electrical conductivity, hardness, wear resistance, machinability and strength can all be modified within rather wide limits.

* Particulate composites based on boron nitride, titanium diboride, and aluminum nitride have properties which are well suited to the requirements of aluminum evaporator boats.

* Boron nitride/titanium diboride composites show an interesting combination of wear resistance and lubricity which may be valuable in a number of grinding and wear resistant applications.

* Boron nitride/boron nitride fibre composite show increased anisotropy due to the effects of fibre orientation during pressing, but little increase in strength or toughness. This is most likely due to fibre degradation during pressing and excessive bonding between fibre and matrix.

* Fibre reinforcement of boron nitride, in non-electrical applications, would be more effective if fibres with greater thermal expansion coefficient and less matrix bonding were used.

* The strength and modulus of boron nitride fibre now produced is much less than that attainable. While the material presently produced is adequate for felt applications, it suffers in reinforcement applications. Work should be done on process improvement to achieve greater strength and moduli.

* Uniaxial cold pressing of prepared powders is an effective and cost effective shaping procedure for boron nitride and boron nitride composites, but care must be taken with these inherently anisotropic powders to control anisotropy and avoid stress-induced lamination and " end capping ".

* Hot pressing is the firing method of choice for boron nitride and boron nitride composites but suffers from the materials problem of weak and unpredictable mold materials suitable for use at or near 2000 degrees C. More effort should be applied to emperical-based design and stress prediction to reduce the production cost of mold breakage.